9-20-2018

The Development of Motor Tandem Axle Module in Series Hybrid Commercial Vehicles

Zicheng Tang
University of Windsor

The Development of Motor Tandem Axle Module in Series Hybrid Commercial Vehicles

By

Zicheng Tang

A Thesis
Submitted to the Faculty of Graduate Studies
through the Department of Mechanical, Automotive & Materials Engineering
in Partial Fulfillment of the Requirements for
the Degree of Master of Applied Science
at the University of Windsor

Windsor, Ontario, Canada

2018

The Development of Motor Tandem Axle Module in Series Hybrid Commercial Vehicles

by

Zicheng Tang

APPROVED BY:

_____

Dr. V. Stoilov

Department of Mechanical, Automotive and Materials Engineering

_____

Dr. E. Lang

Department of Mechanical, Automotive and Materials Engineering

_____

Dr. L. Oriet, Advisor

Department of Mechanical, Automotive and Materials Engineering

September 14, 2018

DECLARATION OF CO-AUTHORSHIP / PREVIOUS PUBLICATION

I.   Co-Authorship

I hereby declare that this thesis incorporates material that is result of joint research, as follows:

Chapter 2 of the thesis was co-authored with Dhruv Bhavsar and Yi Zhang under the supervision of professor L. Oriet and professor E. Lang. In all cases, the key ideas, primary contributions, experimental designs, data analysis, interpretation, and writing were performed by the author, and the contribution of co-authors was primarily through the provision of literature review. Dhruv Bhavsar contributed to the hydric hybrid studies, and Yi Zhang contributed to the hybrid drivetrain optimization studies

I am aware of the University of Windsor Senate Policy on Authorship and I certify that I have properly acknowledged the contribution of other researchers to my thesis, and have obtained written permission from each of the co-author(s) to include the above material(s) in my thesis.

I certify that, with the above qualification, this thesis, and the research to which it refers, is the product of my own work.

II.   Previous Publication

This thesis includes two original papers that have been previously published/submitted for publication in peer reviewed journals, as follows:

Thesis Chapter	Publication title/full citation	Publication status*
Abstract *Chapter [1]* *Chapter [3]* *Chapter [4]* *Chapter [6]*	*Z. Tang, L. Oriet, E. Lang, And Y. Zhang, "Modeling, Control, And Simulation Methods for Series Hybrid Heavy-Duty Commercial Vehicles Powered by Motor Tandem Axle Module," IEEE Transportation and Electrification Conference and Expo (ITEC), 2017, ISBN: 978-1-5090-3904-3.*	*published*

Abstract *Chapter [1]* *Chapter [2]* *Chapter [3]* *Chapter [6]*	*Z. Tang, D. Bhovsar, Y. Zhang, L. Oriet, And E.* *Lang, "The Development of Regenerative* *Braking System for Motor Tandem Axle Module* *in Series Hybrid Commercial Vehicles," Acta* *Mechanica Et Movilitatem, 2017, ISSN 2525-* *9350.*	*published*

I certify that I have obtained a written permission from the copyright owner(s) to include the above published material(s) in my thesis. I certify that the above material describes work completed during my registration as a graduate student at the University of Windsor.

III.   General

I declare that, to the best of my knowledge, my thesis does not infringe upon anyone's copyright nor violate any proprietary rights and that any ideas, techniques, quotations, or any other material from the work of other people included in my thesis, published or otherwise, are fully acknowledged in accordance with the standard referencing practices. Furthermore, to the extent that I have included copyrighted material that surpasses the bounds of fair dealing within the meaning of the Canada Copyright Act, I certify that I have obtained a written permission from the copyright owner(s) to include such material(s) in my thesis.

I declare that this is a true copy of my thesis, including any final revisions, as approved by my thesis committee and the Graduate Studies office, and that this thesis has not been submitted for a higher degree to any other University or Institution.

ABSTRACT

The growing issues of energy shortage and the environmental crisis have resulted in new challenges for the automotive industry. Conventional commercial vehicles such as refuse trucks and delivery vehicles consume significantly more energy than other on-road vehicles and emit more emissions. It is important to make these vehicles more fuel efficient and environmentally friendly. Hybrid powertrains provide a good solution for commercial vehicles because they not only provide optimum dynamic properties but also substantially reduce emissions. For most commercial vehicle powertrains, the internal combustion engine (ICE) is the only power source that provides power to the driveline. The emission reduction faces a limit since a high-powered engine is required to meet the dynamic properties of those heavy-duty vehicles. Also, the high-powered engine cannot avoid operating in low efficient areas due to the fact that these vehicles continually drive at low speeds on designated city routes. However, hybrid powertrains allow commercial vehicles to select lower powered engines because they are equipped with multi-power sources to supply torque together to the driveline. Therefore, hybrid powertrains are a natural fit for commercial vehicles. For this reason, an alternative series hybrid drivetrain system, which contains an electric tandem axle module, has been designed for those heavy-duty commercial vehicles like city transits and refuse trucks. In order to prove the theoretical efficiency and practicability of this application, the modeling methodology for specification of system architectures and hybrid drivetrain control strategies will be provided in this paper with the demonstration of simulation methods and results. [12]

ACKNOWLEDGEMENTS

TABLE OF CONTENTS

LIST OF TABLES

LIST OF FIGURES

LIST OF APPENDICES

LIST OF ABBREVIATIONS

CO   Carbon monoxide

HC   Hydrocarbons

PM   Particulate Matter

GHG   Green House Gas

THC   Total Hydrocarbon

NMHC   Non-Methane Hydrocarbons

DI   Direct Injection

Kg   Kilogram

Km   Kilometers

hp   Horsepower

lb-ft   Pound-foot

L   Liter

rpm   Revolutions Per Minute

psi   Pound Per Square Inch

mm   Millimeter

ICE   Internal Combustion Engine

PHHV   Parallel Hybrid Hydraulic Vehicle

SHHV   Series Hybrid Hydraulic Vehicle

W	Watt
Kw	Kilowatt
AC	Alternating Current
DC	Direct Current
Wh/kg	Watt-Hour Per Kilogram
C/mol	Coulombs Per Mole
v	Volt
NMC	Nickel-Manganese-Cobalt
kWh	Kilowatt Hour
EDLC	Electrochemical Double-Layer Capacitor
back-EMF	Back Electromotive Force
ABS	Antilock Braking System
m/s2	Meter Per Second Squared
kJ/kg	Kilojoules Per Kilogram
cm3	Cubic Centimeter
kg/l	Kilogram Per Liter
1/min	Revolution Per Minute
Nm	Newton Meter
SOC	State of Charge

s   Second

LIST OF SYMBOLS

Symbol	Description
CO_2	Carbon Dioxide
NO_X	Nitrogen Oxides
SO_x	Sulfur Oxides
NO_2	Nitrogen Dioxide
ΔG	Gibbs Free Energy
F	Faraday Constant
n	Number of Charge Carriers
C_e	Equivalent Capacitance
U_{max}	Maximum Voltage of Super-Capacitor
U_{min}	Minimum Allowable Voltage of Super-Capacitor
F_{RR}	Rolling Resistance Force
V_b	Back Electromotive Force Voltage
d	Percentage Discharge Ratio
E_c	Energy of Super-Capacitor
F_{aero}	Aerodynamic Drag Resistance Force
θ	Road Grading

ρ_{air}	Density of Air
C_D	Aerodynamic Drag Coefficient
A_f	Frontal Area
V_f	Final Speed
T_r	Resist Rolling Moment
P	Norm Load
F_r	Equivalent Force
f_r	Rolling Resistance Coefficient
r_d	Effective Radius of the Tire
F_{GR}	Grading Resistance
F_{IR}	Inertia Resistance
F_{trac}	Tractive Force
P_{trac}	Power Rating of the Motor
g	Gravity Acceleration
P_i	Load Power of Engine
g_i	Specific Fuel Consumption
Q_t	Total Fuel Consumption

ρ_{fuel} Mass Density of Fuel

Δt Time Interval of Whole Cycle

η_e Engine Efficiency

T_e Torque Output of Engine

ω_e Output Speed of Engine

$\dot{Q}_t$ Rate of Fuel Consumption

H_{fuel} Heating Value of the Fuel

T_{out} Faraday Constant

P_{out} Power Output

η_{em} Motor Efficiency

ω Angular Speed

R Wheels Radius

T_w Torque on Wheel

T_{out_req} Required Output Torque of Motor

N_{dif} Differential Ratios

V_{oc} Open Circuit Voltage

R_{int}	Internal Resistance
V_t	Battery Terminal Voltage
I_{bat}	Battery output current
P_{batt}	Power Output of the Battery
P_{charge}	Battery Charge or Discharge Power
η_{batt}	Battery Efficiency
E_{max}	Maximum Energy of Ultracapacitor
R_e	Equivalent Series Resistance of Ultra capacitor
P_{max}	Maximum Power of Ultra capacitor
SOC_i	Initial State of Charge
t	Time
A	Amp-Hour

CHAPTER 1

Introduction

The civilization of human society has dramatically changed since Karl Benz introduced the first petrol powered automobile to the world in 1885. Automobiles were one of the main contributing factors boosting modern industrial economy progress. However, the negative effects of vehicle popularization like air pollution, climate change, and energy sustainability have also been brought to the table along with the benefits. Therefore, reducing emission and improving fuel efficiency have become the focus of current automotive industries, especially when it comes to the heavy-duty commercial vehicles. New alternative energy source, such as vehicle electrification, are the irresistible general trend to minimize the load of Internal Combustion Engine.

1.1 Objectives

The main objective of this research was to design a new series hybrid drivetrain system for city operated heavy duty commercial vehicles, which contains a dual diesel engine generator and an electric motor tandem axle module. This tandem axle module is propelled by a dual-rotor electric motor, which provides the possibilities to induce brake energy recovery system into this application. Meanwhile, due to the series hybrid configuration, the dual diesel engines could operate with optimized engine speed. The modeling methodology for specification of system architectures and hybrid drivetrain control strategies are also provided along with the demonstration of simulation methods and results to prove the theoretical efficiency and practicability of this application.

1.2 Environment Impacts by Automobiles

According to Winston and Virginia, automobiles play a major role in causing air pollution and global warming based on a large and growing share of pollutants greenhouse gas emissions worldwide [1].

There are three main types of air pollutants created by vehicles that could bring negative impact on air quality. The first type of pollutants like carbon monoxide (CO) usually occurs when the combustion process of the fuel is incomplete. In this case, carbon monoxide (CO) is produced because of insufficient air. When inhaled carbon monoxide, human body will experience headache, dizziness, vomiting, and nausea. Certain long-term health problems like heart disease and lack of red blood cells are more likely to occur after breathing high levels of carbon monoxide over long periods of time. However, this does not mean that the complete combustion process of the fuel is clean. The major portion of air pollutions listed below are actually from the chemical processes during complete combustion, which depends on different types of fuels, engines, and environment conditions.

- **Carbon dioxide (CO_2):** It is also defined as a greenhouse gas that contributes to global warming.
- **Nitrogen oxides (NOx):** The lung function can be damaged by this irritant gas.
- **Sulfur oxides (SOx)**: Sulfur dioxide (SO_2) is a harmful compound to human respiratory system and mucous membrane.

The final type of pollutants is formed by reactions of vehicle emissions in the atmosphere. The ground level ozone (O_3), which is capable of damaging humans' pulmonary function, respiratory system, and immune system, can be generated by

emissions of both hydrocarbons (HC) and nitrogen oxides (NOx). Nitrogen oxides (NOx) can also form nitric acid by reacting with water. In same case, sulfur oxides (SOx) forms sulfuric acid and sulfate aerosols in the atmosphere that contributes to acid rain and particulate matter (PM) pollution respectively. [1] Meanwhile, particulate matter (PM) is another unneglectable pollutant from vehicle emissions. Based on the size of particulates from vehicle emissions, Total Suspended Particulates (TSP) is defined into two categories: PM2.5 and PM10, which refers respectively to particulate matters with less than 2.5 μm diameter and 10 – 2.5 μm diameter.

Since the combustion process of the engine is the source of the vehicle emissions patterns, the pollutants vary with different fuel type. Emissions from petrol cars contain higher level of carbon monoxide (CO) and hydrocarbons (HC) when compare to a diesel car. Meanwhile, lead only occurs in emissions of petrol because of leaded gasoline. However, emissions of nitrogen oxides (NOx) and particulate matter are much higher in diesel cars.
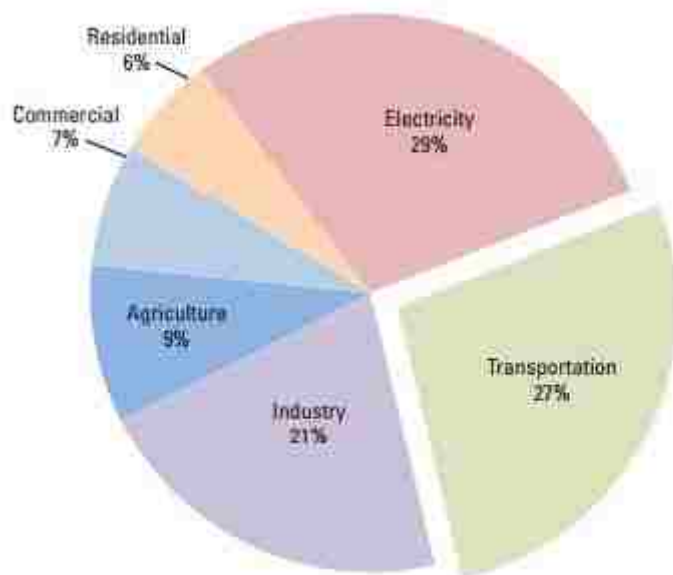
Figure 1. Share of U.S. Green House Gas by Sector, 2015 [3]

As demonstrated above, all kind of vehicle emissions contain serval harmful pollutants, which can cause series damages to either environment or human bodies in long term exposure. The research of David Mage and Olivier Zali indicates that there are 3.4 billion trips are taken by vehicle daily in major cities around world and at least 120 million peoples in those cities spend a working day in roadsides settings, which means large numbers of people being exposed to high levels of pollutants has become a significant problem. [2] Plants are damaged by acid rain caused by nitrogen oxides (NO_2); and sun's ultraviolet radiation becomes more harmful because of deterioration of ozone. According to Figure 1. from United States Environmental Protection Agency, 27% of total U.S. Green House Gas (GHG) emissions in 2015 are from transportation, which includes cars, trucks, commercial aircraft, and railroad. Within the transportation sector, 83% of emissions are from cars and trucks. [3] All of these greenhouse gas (GHG) emitted by automobiles prevents heat dissipation in the atmosphere, hence global temperatures start to increase, which is shown on Figure 2.
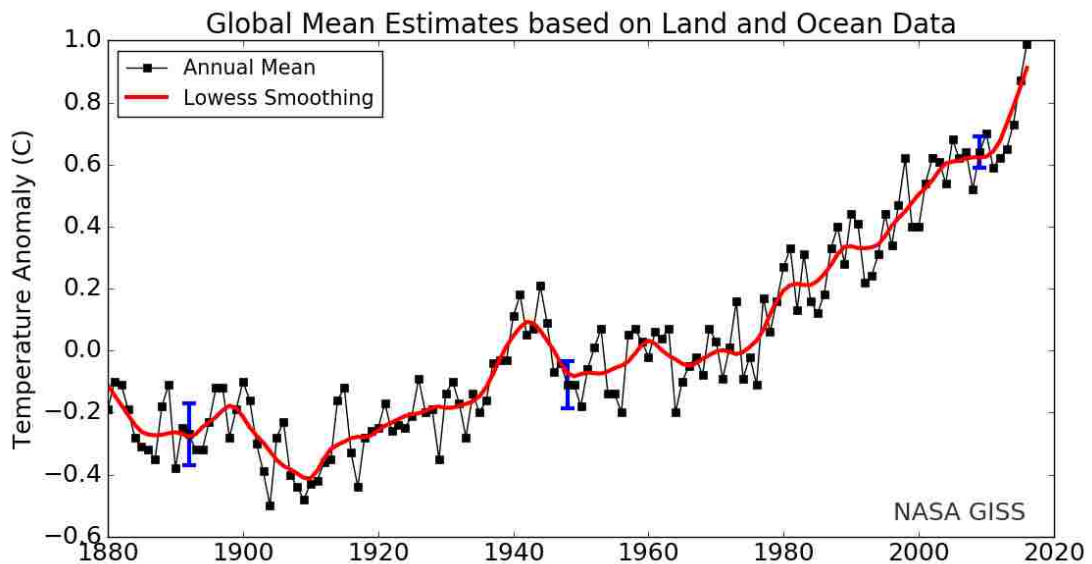
Figure 2. Global Annual Mean Surface Air Temperature Change [4]

1.3 Emissions Regulations, Improvements, and Concerns

Since the emissions of vehicles has become the major contributor to the negative impacts on environment, societies urge automakers to bring cleaner and more fuel-efficient vehicles on the markets. With this momentum for automotive industrial building globally, more countries and regions are willing to enforce and develop more energy-efficiency policies for the transport sector. For instance, vehicles in Europe had to reach the requirements of the European emission standards and the regulation of carbon dioxide emissions. The European emission standards are known by a 'Euro' sign followed by Arabic or Roman numbers, and mandate the acceptable limits for vehicles emissions of nitrogen oxides (NOx), total hydrocarbon (THC), non-methane hydrocarbons (NMHC), carbon monoxide (CO) and particulate matter (PM). As Table 1. and Table 2. from Kajsa Lindqvist shows, the Euro standard has been progressively and frequently tightened for the emission limits of both light-duty and heavy-duty vehicles in past 20 years. [5]

	NOx		THC [1]		THC [1] + NOx		PM		PN [2]	
	Diesel	Petrol	Diesel	Petrol	Diesel	Petrol	Diesel	Petrol	Diesel	Petrol
Euro 1 1992.07	-	-	-	-	970	970	140	-	-	-
Euro 2 1996.01	-	-	-	-	700/900 [3]	500	80-100	-	-	-
Euro 3 2000.01	500	150	-	200	560	-	50	-	-	-
Euro 4 2005.01	250	80	-	100	300	-	25	-	-	-
Euro 5a 2009.09	180	60	-	100	230	-	5	5	-	-
Euro 5b 2011.09	180	60	-	100	230	-	5	5	6×10^{11}	-
Euro 6 2014.09	80	60	-	100	170	-	5	5	6×10^{11}	-

Table 1. Emission standards for Light-duty vehicles in mg/km [5]

	NOx (g/kWh)		THC [1] (g/kWh)		NMHC [2] (g/kWh)		PM (mg/kWh)		PN (#/kWh)	
	Diesel	Gas/Petrol	Diesel	Gas/Petrol	Diesel	Gas/Petrol	Diesel	Gas/Petrol	Diesel	Gas/Petrol
Euro I 1992	8.0	-	1.23	-		-	360/612	-	-	-
Euro II a 1996.10	7.0	-	1.1	-		-	250	-	-	-
Euro II b 1998.10	7.0	-	1.1	-		-	150	-	-	-
Euro III 2000.10	5.0 [3]	5.0	0.66 [4]			0.78	100/160 [5]	-	-	-
Euro IV 2005.10	3.5 [3]	3.5	0.46 [4]			0.55	20/30 [5]	-	-	-
Euro V 2008.10	2.0 [3]	2.0	0.46 [4]			0.55	20/30 [5]	30	-	-
Euro VI 2013.01	0.4/0.46 [6]	0.46	0.13/0.16 [6]			0.16	10/10 [6]	10	$6 \times 10^{11}/8 \times 10^{11}$ [6]	-

Table 2. Emission standards for heavy-duty vehicles [5]

As a result of high-pressure policy, major automobile companies have brought a lot of new technologies and methods on the table to make these vehicles more fuel efficient and environmentally friendly. Catalytic converter, an exhaust emission control device, was one of those technologies popularized due to emissions limit policies. Therefore, since the main focus of automotive societies has switched to emission reduction and fuel saving, the preliminary results of air pollutant reduction were encouraging. Even with the high growth of vehicle sales, air pollutant from the emissions transportations has been decreasing for past decades. [6] The indexes of most key air pollutant emissions from U.S. transportation in Figure 3. are experiencing a downward trend from 1990 to 2013.
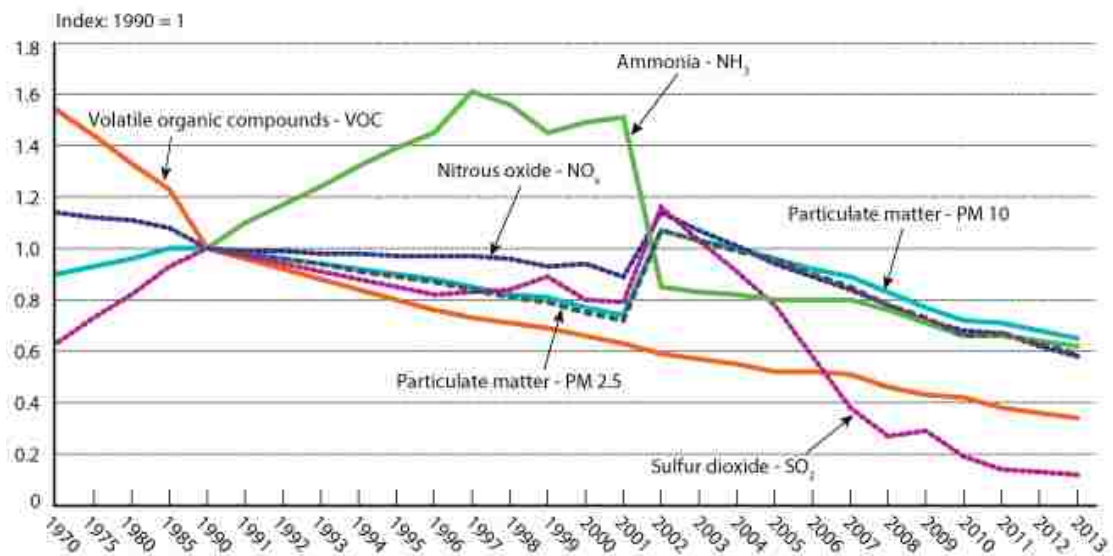
Figure 3. Indexes of Key Air Pollutant Emissions from U.S. Transportation: 1970-2013 [7]

However, there are no standards for limits on CO_2 emissions of heavy-duty vehicles, which means these commercial vehicles with heavy engine load missions are consistently consuming tremendous amount of fuel and producing tons of greenhouse gas (GHG) around world. The heavy commercial vehicles like refuse trucks and city

6

transit vehicles averagely travel around 40000 kilometers per year and consumes 80-100 liters per hundred kilometers. [8] Meanwhile, when operated at a daily stop-go route in the city, the heavy-duty commercial vehicles waste a tremendous amount of energy during braking and idling, which also result in a highly inefficient driving cycle. [9] When we break down the U.S. Green House Gas (GHG) emissions by transportation sectors for 2015 in Figure 4. medium- and heavy-duty trucks account for 23% of greenhouse gas (GHG) emissions, almost half of the light-duty vehicles. Compare to all these fancy alternative drivelines been used on new passenger cars, it should be clearly to state that heavy-duty vehicles deserve more focus from the automotive industrials to improve the efficiency and emissions of their drivelines.
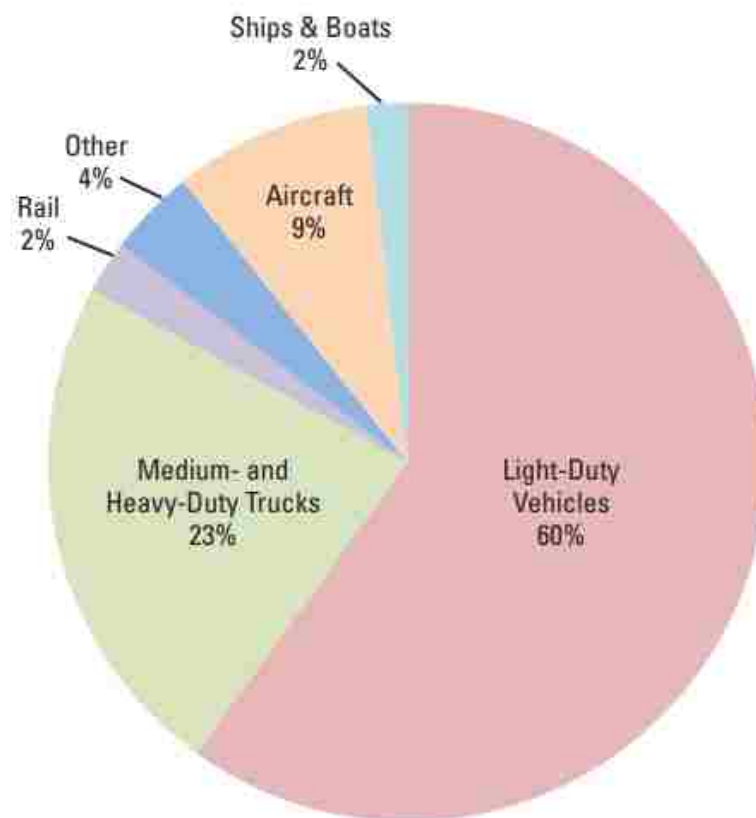
Figure 4. Share of U.S. Transportation Sector GHG Emissions by Source, 2015 [3]

1.4 Alternative Driveline and Vehicle Electrification

In order to reduce fuel consumption and greenhouse gas (GHG) emissions of vehicle, certain alternative drivelines have been introduced to todays' automotive industrials. Even most of the innovations are for the passenger vehicles, there are still few that has been developed for the heavy-duty vehicles.

The highly efficient internal combustion engine is one of most common pathways that contribute to improve fuel consumption and greenhouse gas (GHG) emissions. One approach that is been rapidly utilized in the market is engine downsizing, which can be achieved by better fuel vaporization from fuel direct injection (DI) and turbocharging. The energy losses from engine friction and torque conversion are unneglectable when maximizing driveline efficiency. Hence, redesigning drivetrain with more efficient transmissions and improving lubrication for better overall design in the engine are the solution right now for the better efficiency. [9] Meanwhile, new systems like engine start-stop can automatically stop and start the engine based on the operating conditions of vehicle, so fuel supply is able to be cut off when vehicles are stopped in traffics. This system allows the internal combustion engine of the vehicle to operate in a more fuel efficiency control strategy because of the no fuel consumptions for idle stop. It is useful to the vehicle that travels in city condition routes, however, all the improvements mentioned above have limitations and draw backs. Additional wear may be applied to the engine for the long-term use of engine start-stop, and saving of the fuel is not significant for low traffic routes. Therefore, to further enhance the improvements of clean technology on vehicles, alternative energy sources are brought on the table.

Alternative energy sources include non-petroleum-based fuel like hydrogen, biofuels, and natural gas; and electricity. Due to its greater reliability, vehicle electrification and hybridization have become the most common applications in recent years. Among the vehicle electrification applications, electric vehicles are the cleanest one, since the 20% of the electricity is generated from renewable energy sources and 18% of the electricity is generated from nuclear in North America which is showed in figure 5. [10] However, the short range, lack of recharging points, heavy weights, and battery problems of electric vehicles have not been fully solved, so hybrid technology that utilizes both electric motor and internal combustion engine is developed as a transitional function for electric car. The hybrid system satisfies the improvement of these types of vehicles' fuel economy and has less weight effects caused by batteries and other power storage devices. [11] Since the hybrid drivetrain provides the possibilities of inducing the braking energy recovery system by utilizing electric drive system, it is considered as one of the best choices for the city operated heavy-duty commercial vehicles. [12]
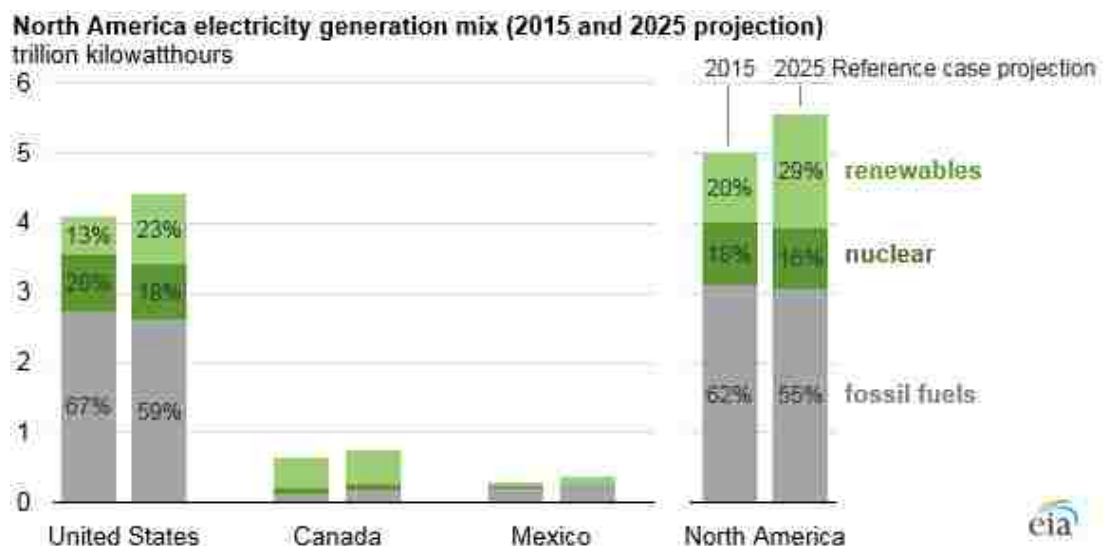
Figure 5. North America electricity generation mix [10]

CHAPTER 2

Literature Review

This chapter provides an overview of the relevant literature and summary of the research on conventional heavy-duty commercial vehicles, hybrid vehicles, and brake energy recovery systems.

2.1 Conventional Heavy-Duty Commercial Vehicle

Heavy duty commercial vehicles are classified differently in different countries, but most of counties defined this type of vehicles by weight. So, the weight of heavy-duty commercial vehicles, which is average 23000 Kg of curb weight in North America, shapes the characteristic of their powertrains and chassis. The reason of the high weight is because of the main job of the heavy-duty commercial vehicles, which is moving varieties of objects. The focus of this thesis will be on city operated heavy duty commercial vehicles like city transits, furniture delivery trucks, and refuse trucks.

2.1.1 Engine

Most of the heavy-duty commercial vehicles are using diesel engines, which have better lubrication properties, higher compression ratios and energy density. According to Rachel M. Zoyhofski, there are 55% of the energy turn into work by diesel engines, while gasoline engines can only convert 35%. [13] For the vehicles are required to travel 40000 kilometers per year and normally carry legal payload of about nine tons, the more durable diesel engines provide an ideal propulsion to system.

Cummins X15, one of the top diesel engines, has been widely used for fire trucks in North America. As Table 3. demonstrated, this inline 6 diesel engine has 505 to 600 hp and 1850 lb-ft of peak torque with 14.9 L displacement and 32,000 psi Injection Pressure. Based on the Figure 6. the X15 torque & horsepower curves, this

engine can reach peak braking horsepower at engine speed of 1850 rpm and peak torque

between engine speeds of 1100 rpm and 1700 rpm. [14]

Advertised Horsepower	505-600 hp	362-447 kW
Peak Torque	1850 lb-ft	2508 N•m
Configuration	Inline 6	
Displacement	912 cu in	14.9 L
Lube Oil Capacity	44 qt	41.6 L
Biodiesel Compatibility	Up to B20	
Engine Braking Horsepower	Up to 600 hp @ 2100 rpm	
Idle Speed	600-800 rpm	
No Load Governed Speed	2130 rpm	
Engine Weight (Dry)	2,964 lb	1,344 kg
Aftertreatment Weight*	173-211 lb	78-96 kg
Injection Pressure	32,000 psi	

Table 3. X15 Performance Series for Fire & Emergency (2017) Specifications [14]
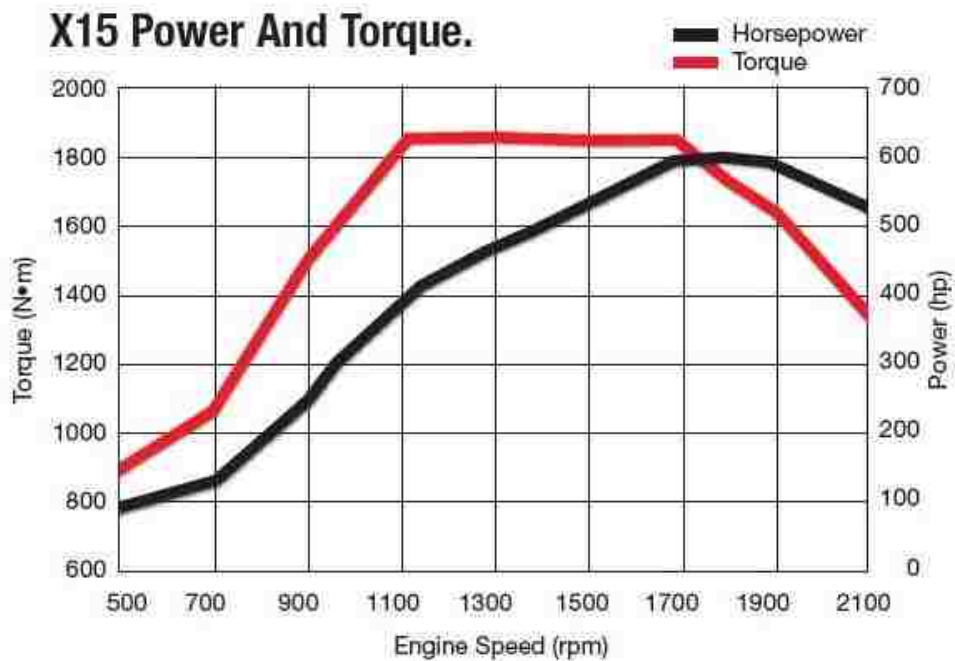
Figure 6. X15 Performance Series for Fire & Emergency Torque & Horsepower

Curves [14]

2.1.2 Drivetrain

The drivetrains of the heavy-duty commercial vehicles are varied by the distinct functions of the trucks. Generally, they have similar but simpler structures of passenger vehicles' drivetrains. There are two typical heavy tractor configurations, which are 4x2 and 6x4. The 4x2 consists of four wheels and only two of them are used to propel the vehicle, and the 6x4 has 6 wheels and 4 of them propel the vehicle. [15] The Figure 7. provide an example of 6x4 drivetrain from Prima LX 4923.S, where can be showed that torque is transferred from engine to a 9-speed gearbox by a 430mm diameter clutch, and two cutaway differential carriers pass the torque to wheels trough tandem axles.

Figure 7. Prima LX 4923.S Drive Train. [16]

The gearbox used in Prima LX 4923.S is a Tata G 1150 OD 9-speed Gearbox which deals with input torque of 1150 Nm with a centre distance of 125 mm. To achieve the better start ability and maneuverability, the gear ratios indicated in table 4. are used.

Table 4. Gear ratio of Tata G 1150 OD 9-speed Gearbox [16]

Crawler	1st	2nd	3rd	4th	5th	6th	7th	8th	Rev
12.868	9.139	6.725	4.903	3.571	2.559	1.883	1.373	1.00	13.399

A cutaway differential carrier is displayed in Figure 8., where the black line represents the torque transfer flow. When the power divider is locked, torque is delivered from input shaft through helical gears to ring gear and differential side gears, which will transfer the torque to each wheel trough the drive axle. When the power divider is unlocked, torque is delivered from differential. [17]
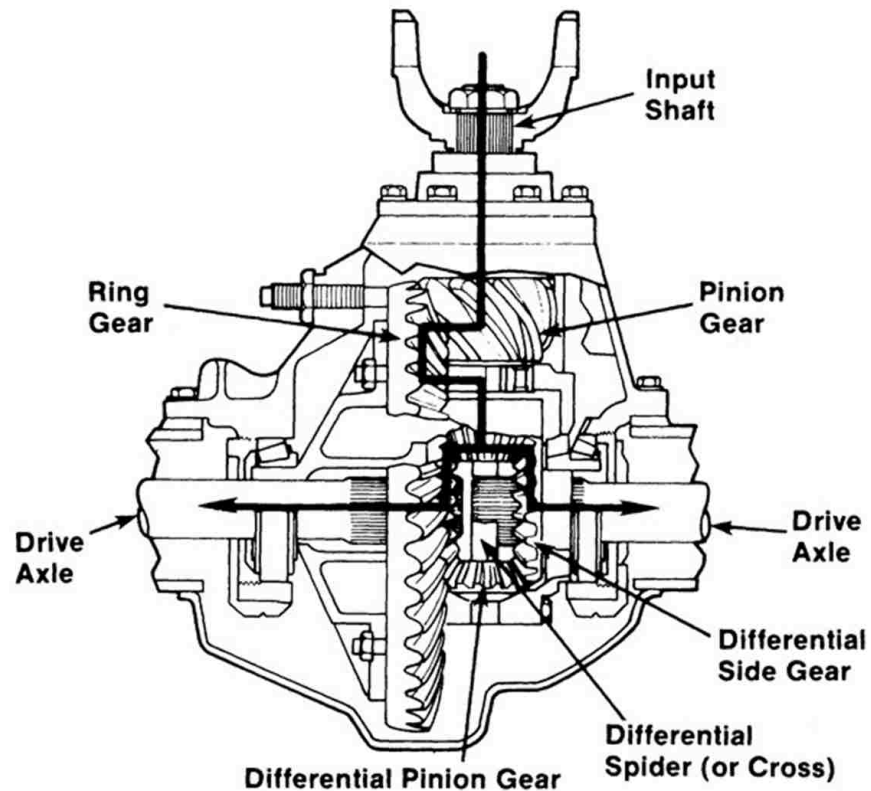
Figure 8. Cutaway Differential Carrier [17]

In Figure 9. the tandem drive axles have front axle and rear axle connected by a propeller shaft. So, torque provided by differential is delivered from propeller shaft to rear axle, when the power divider is unlocked. Otherwise, torque will go through the propeller shaft directly to rear axle. [17]
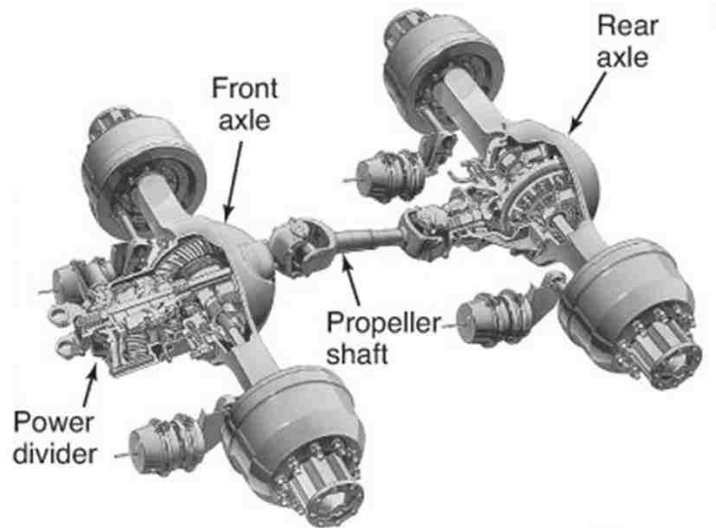
Figure 9. Tandem Drive Axles [17]

2.1.3 Frame

The typical structure of a truck frame is based on two parallel rails held together by riveted and bolted cross members, which is well known as a ladder frame. For a 6x4 truck, the frame is sited on a straight front axle by a working leaf-spring suspension and tandem drive axles by a bogie suspension. The materials of most frames are steels or aluminum; and the vehicle's floor plan will be placed above the frames. It has ability to provide better beam resistance and worse torsional resistance, which makes the frame more applicable to heavy trucks rather than passenger cars.

In Figure 10. the configuration of the MAN CLA 26.280 6x4 BB Tipper's chassis is presented as the example of the typical 6x4 truck chassis. According to MAN's specification brochures, the L09 wheelbase is 3875mm, the L02 is rear axle spacing which is 400mm, L10 is front overhang which is 1293mm, L11 is rear overhang which is 1300mm, and L43 is chassis length behind cab of 5025mm, so the overall length of the chassis is 7257mm and foremost point of body from front axle is 850mm.
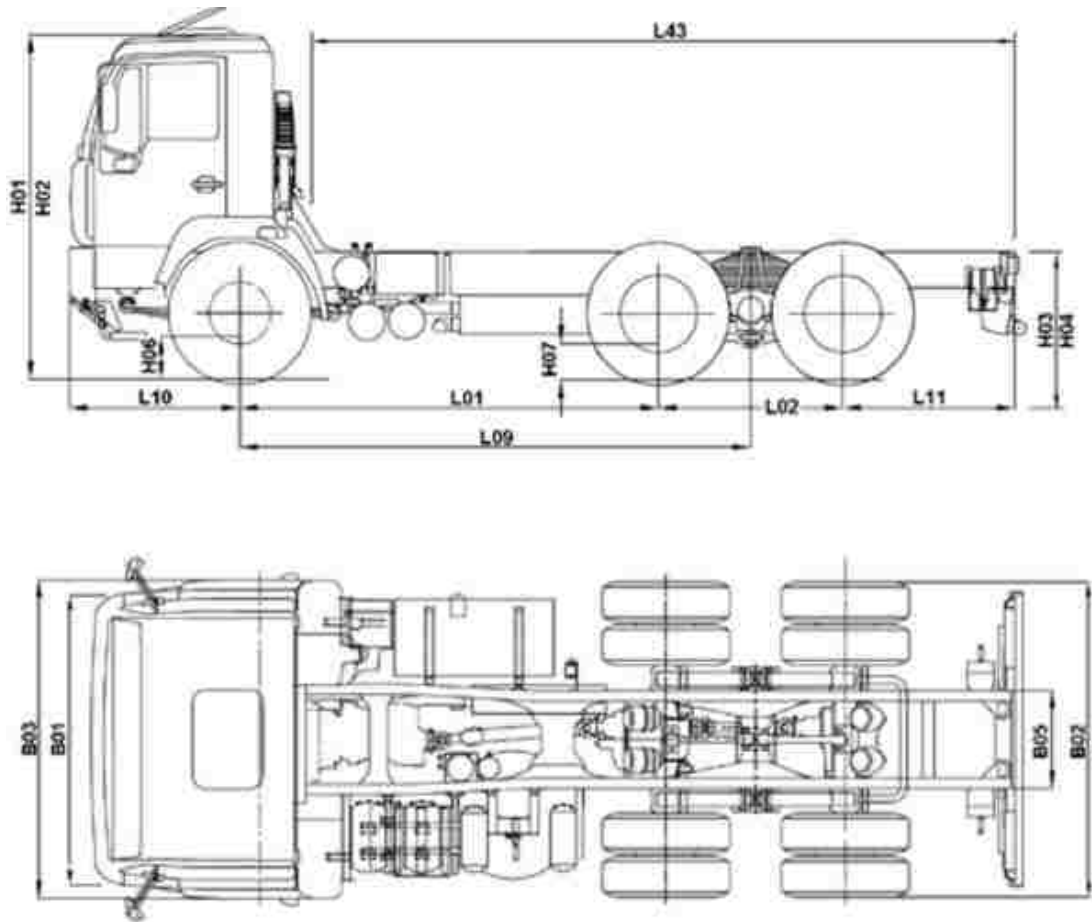
Figure 10. Man CLA 26.280 6x4 BB Tipper Chassis [18]

2.2 Hybrid Vehicle

As mentioned above the hybrid systems have become the major solution for the auto industries, whose desire is to offer the 'greener' trucks to the world, so researches have been conducted to indicate the characteristic, benefits, and drawbacks of different hybrid technologies. In this section, hybrid vehicles are categorized and reviewed in three main classes: series, parallel, and hydraulic.

2.2.1 Parallel Hybrid Vehicle

The parallel hybrid is the most common hybrid drivetrain for current passenger vehicles, which usually has an internal combustion engine and an electric motor directly joined at an axis by a transmission shaft. The internal combustion engine is powered by

15

fuel or diesel and the electric motor is powered by battery can propel the vehicle by the engine alone or by the motor alone, or by both together at same rotational speed and torque. The internal combustion engine also used as a generator which convert mechanical energy to electrical energy that charges the battery. [11] Since the parallel hybrid has a mechanical connection between each power sources, the transmission is required in this drivetrain system like shown in Figure 11. There is a clutch between the engine and transmission to allow electric launch without starting the engine.
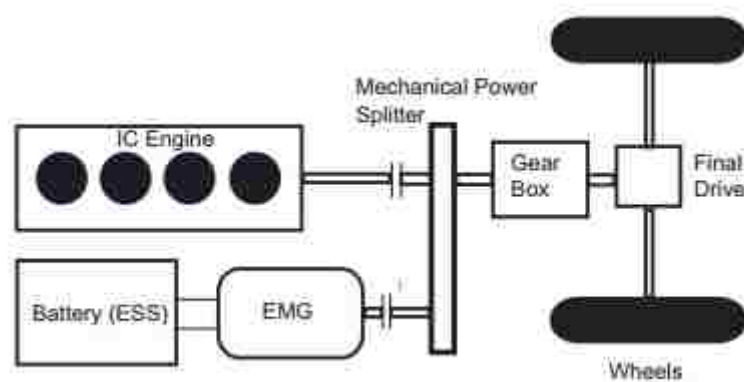
Figure 11. Topology of a parallel hybrid electric vehicles [19]

The better drivetrain efficiency is the main advantages of parallel hybrid electric vehicles because of controllable couple operation of the internal combustion engine and the electric motor, which allow varied capacities of the engine and scalable electrical power system with same drivability of the vehicle. [19] However, due to the most parallel hybrid vehicles only need one electric motor with a low power rating, regenerative braking system will be less efficient and more mechanical dependable in parallel hybrid.

2.2.2 Series Hybrid Vehicle

Figure 12. shows the component configuration of a series hybrid system. The internal combustion engine (ICE) only drives the electric generator, which recharges the larger battery packs or propel the wheels by the electrical motor through Electric Power Splitter. Therefore, there is no mechanical connection between the ICE and the wheels. The ICE converts thermal energy into the mechanical energy, and thereafter, in the generator, turned into electric energy, used to charge the battery which in its turn supplies the electric traction motor. [20]
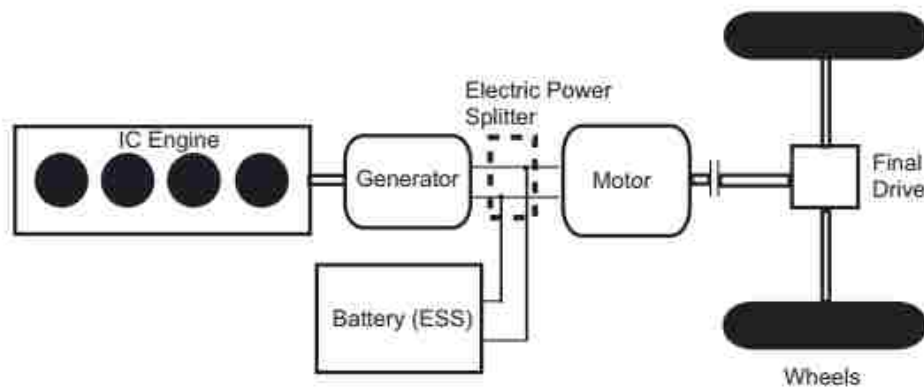
Figure 12. Topology of a series hybrid electric vehicles [19]

Due to more energy conversions, which contributes to high energy loss, the overall efficiency of the series hybrid power train is significantly affected. A heavier battery with higher capacity is unavoidable for series hybrid vehicles, since the internal combustion engine only works as an electric vehicle range extender. However, the impact of the extra batteries' weight plays a less significant role for heavy duty commercial vehicles like garbage trucks, which weighs about 13 to 28 tones. Meanwhile, instead of operating over a wide variety of engine speeds, the optimized engine speed can also be run continuously even during the stop-start traffic. In this case, the series hybrid power train system can provide an optimal operative strategy for fuel

efficiency and exhaust emissions. [11] Moreover, the electric motors of the series hybrid vehicle are required to handle peak power, which means they generally have higher power rating. Therefore, the series electric hybrid vehicles are more suitable for brake energy recovery system then parallel electric hybrid vehicles.

2.2.3 Hydraulic Hybrid

Hydraulic hybrid is an important branch of hybrid technology especially when it comes to heavy duty commercial vehicle. It has been widely utilized and developed by automotive manufactory and institutions. The hydraulic motor and/or pump is the secondary power source in hydraulic hybrid vehicle, which is also similar to hybrid electric vehicles' electric motor. [21] Therefore, hydraulic hybrid can be further classified into series, parallel and series-parallel, based on their power train layout.

In parallel hydraulic hybrid, the internal combustion engine is the prime power source, and produces torque to the wheels through the transmission, shaft, and differential, like Figure 13. The hydraulic components are used as energy bumper to provide assistance to vehicle's stopping and accelerating.
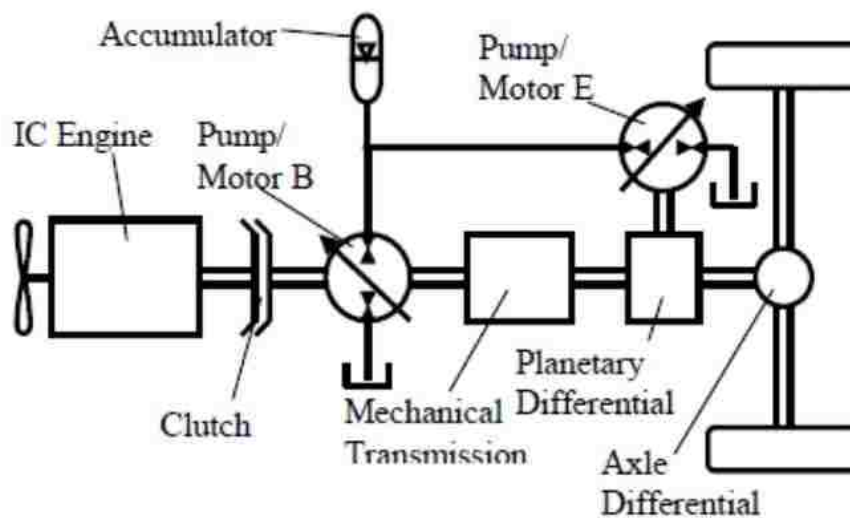
Figure 13. Parallel Hybrid Hydraulic Vehicle (PHHV)

In series hydraulic hybrid configuration in Figure 14. from my colleague Dhruv Bhavsar, the internal combustion engine only connects to a pump to store energy into an accumulator, which uses high pressure to propel the vehicle.
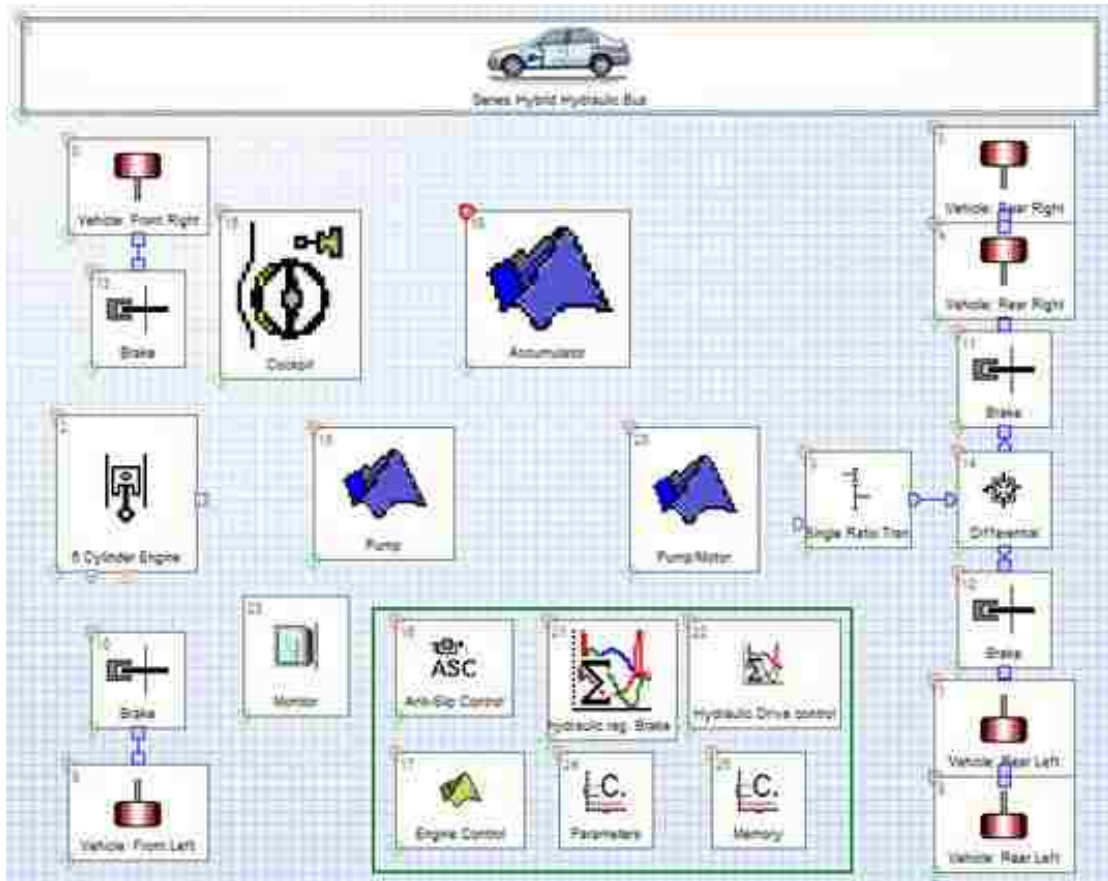
Figure 14. Series Hybrid Hydraulic Vehicle (SHHV) [21]

Both series and parallel hydraulic hybrids are capable of regenerative braking. According to my colleague Dhruv Bhavsar, 'when compare to electric hybrid vehicles, high efficiency of the hydraulic pump/motor and high-power density of accumulator at approximately 500-1000 W/kg contribute in a more effective regeneration of energy while deceleration. However, comparatively low energy density of accumulator creates special challenge and requires novel approaches in the development of supervisory control strategy.' [21] Based on above information, the series hybrid electric drive train is more suitable for heavy duty commercial vehicles for city operations.

2.3 Regenerative Braking

The brake energy recovery system, also referred to the regenerative braking system, is of vital importance to the energy efficiency of the series hybrid commercial vehicle, especially for the frequently stop-go vehicles like garbage truck. [11]

In a typical conventional braking, disc brake is most common braking system for current automobiles to slow the rotation of the wheels by the friction between brake pad and brake rotor. In this case, the friction pads are pressed into brake disc by the piston of the fixed caliper, which contains hydraulic force from brake fluid cylinders. Another type of braking, known as drum brakes, slows the rotation of the wheels by pressing the friction pad to the inner surface of drum of the wheel. Both of the traditional braking systems turn most of the kinetic energy of the moving vehicle into a tremendous amount of heat energy by friction. [22] Therefore, the recovery of vehicle kinetic and potential energy in conventional braking systems becomes the one of major development in hybrid vehicles. [11]

As mentioned before, the characteristic of electric motor in hybrid electric vehicles is enabling to allow the bi-directional power flow, which helps the braking system to seize the kinetic energy as electricity by using the motor as a generator. The electricity from generator can be saved in an energy storage device like a battery or ultra-capacitor. According to Lester J. Erlston's illustrations, "a division of a vehicle's total kinetic energy, based on a realistic assumption that 50% of the available kinetic energy from a braking or slowing event is able to pass through the recovery system, and shows that a) 40% of this energy will be stored in the batteries for future use, and b) that the foundation brakes will experience a load reduction from 95% to 45% of the total kinetic energy for a comparable non-kinetic energy recovery system braking event,

the other 5% being for losses due to aerodynamic drag and road-to-tire friction." [23]

When the hydraulic hybrid vehicle starts braking, the momentum of the wheels impels the pump to pressurize fluid into the accumulator. This highly pressurized fluid in accumulator drives the pump to accelerate vehicle after braking. Around 75% of the friction braking energy are regenerated by this process. [24]

CHAPTER 3

Design of The Series Hybrid Commercial Vehicles' Drivetrain

The design and development of a new series hybrid commercial vehicles drivetrain, which is powered by Dr. Oriet's inventions of "Structural Electric Tandem Axle Module" and "Series Hybrid Generator", which provides the fundamental structural of this series hybrid powertrain, are presented in this chapter. The details of battery and ultra-capacitor are also explained with brake energy recovery system.

3.1 Configuration of Drivetrain

As Figure 15. demonstrated, the series hybrid drivetrain contains a dual-diesel engine generator, which is invented by Dr. Oriet, consists of two turbo diesel engines connected by an electric generator with two hydraulic internal wet-disk clutches between. The power generated by the dual diesel engine only is delivered to each components of the vehicle through mechanical and electrical paths, which are respectively represented by blue and red lines. The dual-diesel engine provide power through the mechanical path to the electric generator to produce the alternating current (AC) as the function of the range extender. The alternating current (AC) can be converted to direct current (DC) by a convertor, then dispatched by the controller unit through two electrical paths to either charge the battery or drive the dual rotor electric motor. The dual rotor electric motor transfers the electrical power to mechanical power by interacting electromagnetic field patterns from direct current (DC) and outer rotor's permanent magnets. Thus, the torque produced from the electric motor is mechanically delivers to the wheels through the differentials on each tandem axle. When vehicle starts braking, the dual rotor electric motor can also work as a generator to recovery the braking kinetic energy as electric power, which will be stored in ultra-capacitor first,

then either slowly charge the battery or power the electric motor based on the State of Charge (SOC) of the battery. [12]
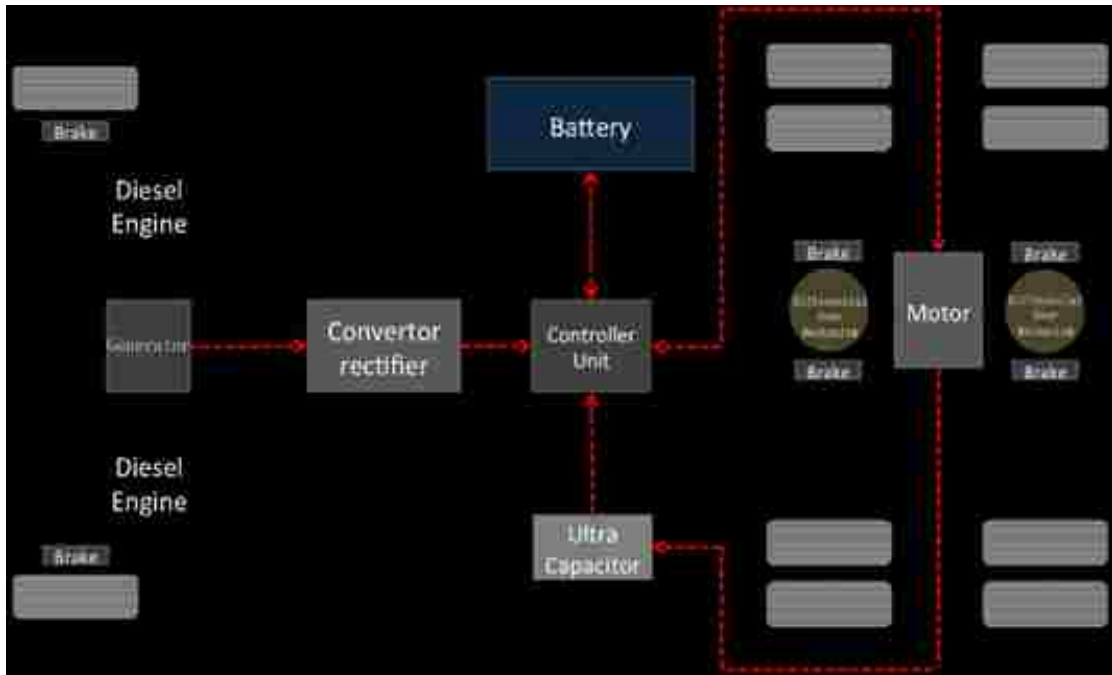
Figure 15. Series Hybrid Drivetrain Block Diagram [11]

3.2 Dual Diesel Engine Generator

This series hybrid generator has an outer rotor and inner rotor with generator winding connected to two identical diesel engines by two hydraulic internal wet-disk clutches, which will allow them to rotate in opposite direction. This dual diesel generator as Figure 16. showed will be working as a range extender in this application, which means that the diesel engines can be continuously run at the optimized engine speed even during the stop-start traffic. According to Dr. Oriet, "the analysis of that drive shows that this selective use of the engines can enable a vehicle to achieve significant fuel economy improvements in comparison to improvement which is likely to be obtained in engines and engine controls through use of conventional single-engine/powertrain design." [25] [12]
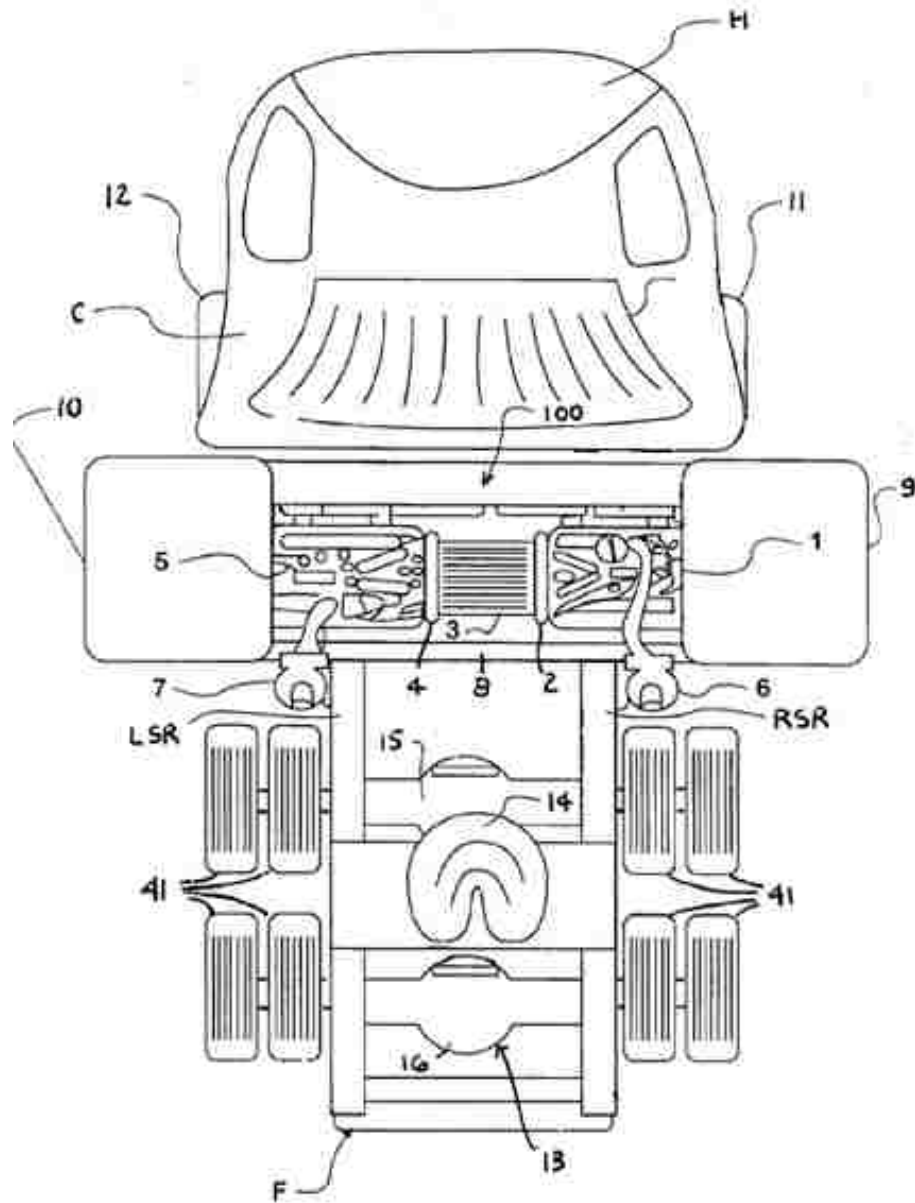
Figure 16. Structural Electric Tandem Axle Module and Series Hybrid Generator by

Dr. Oriet [25]

3.3 Electric Motor Tandem Axle Module

The core of this design is based on Dr. Oriet's invention of "Structural Electric

Tandem Axle Module", which is an electrical powered tandem axle that provides torque

by a dual-rotor motor in the center. [11]
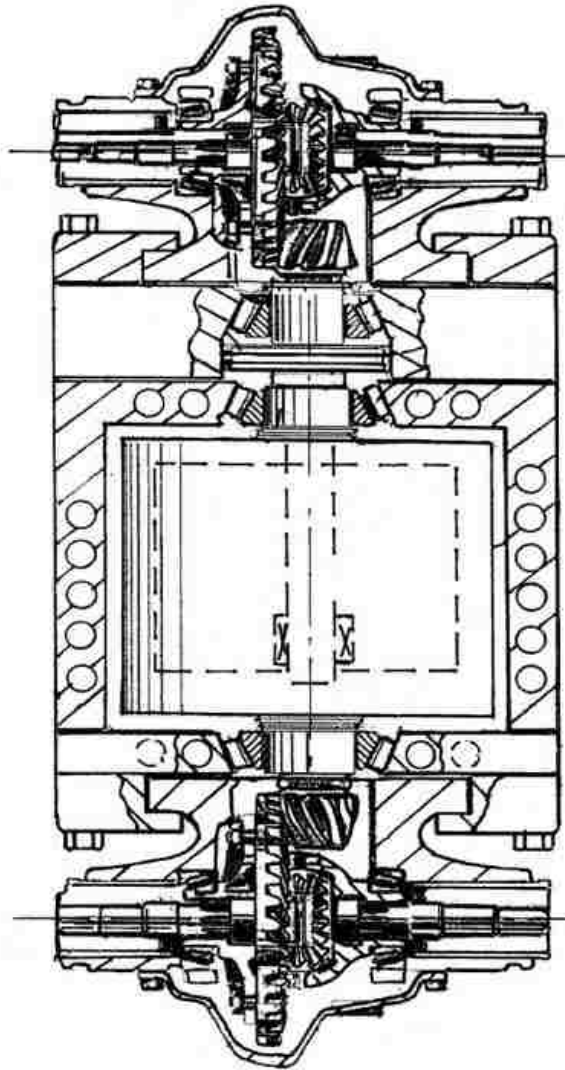
Figure 17. Electric Motor Drive of Structural Electric Tandem Axle Module by Dr.

Oriet [26]

Normally, commercial trucks like refuse vehicles have a chassis, which is a combined of pair of frame rails cross joined with front and rear axles that clamp to the suspensions. The internal combustion engine of the trucks provides the torque through the driving shaft located as a longitudinal axis from front to rear. As we know, the torque delivered to the wheels by the engine is applied to the frame at the same time. Meanwhile, there are also appreciable amount of torque transferred from the driveline to the frame by the suspension system due to the rough road. This condition can cause

repeated twisting to the torsional rigid components that are attached to the frame rails, and half of torque produced by the engine is lost. [26] In order to change the repeated torsion absorption into an exploitable condition and improve the fuel efficiency of commercial trucks, Dr. Oriet came up the idea of a structural electric tandem axle module as Figure 17. This module is propelled by a dual-rotor electric motor, which has two rotors to deliver the same torque from rotor shafts' bevel pinion gears to the differential gears that connected to front and rear tandem axles' wheels. Instead of wasting the half of the rotational mechanical torque as strain on frame, the module perfectly exploits the characteristic of dual rotors motor, which results in better handling and a more efficient driveline. Moreover, there is reduction of torque applied to the frame side rails, the weight of chassis is able to be reduced. At same time, the utilization of the electrical drive system induced in the hybrid system into this application, which endows the brake energy recovery system a more applicable platform. [11]

3.4 Battery

The battery is of vital importance to hybrid electric vehicle, since the energy capability of the battery determines the maximum power limitation. To design a suitable battery packs for this application, the types, principle, and properties of the battery cells are specified by key attributes, which are the cycle life, specific energy density, specific power, and cost of manufacturing.

There are several types of battery that been used in real world applications, and the most used options for automotive industries are the following: lead acid, nickel metal hydride, and lithium-ion. Since the series hybrid vehicles require high specific power and high energy storage capacity, the low energy density character of lead acid

battery, which indicates its low energy storage capacity means it is not suitable for this application. The comparisons of nickel metal battery and lithium-ion battery clearly stated that lithium-ion battery provides higher energy and power density with lighter weight and long cycle life. Therefore, the lithium-ion battery which has over 100 Wh/kg energy density been selected in this application.

The lithium-ion battery's working principles are based on three aspects; anode, electrolyte, and cathode. According to Vishal Mahajan, 'When two chemicals contact with each other, they react with each other based on their tendency to gain or lose electrons. An electrochemical cell is designed in such a way that one electrode will undergo oxidation while the second electrode will undergo reduction when both the electrodes are connected by external electronic path provided by anode and cathode.' [28] In this case, potential difference between each ends of the external electronic path is known as the open circuit voltage, which can be evaluated by Eq.1. where ΔG is Gibbs Free energy, F is Faraday Constant valued as 9.65 x 10^4 C/mol, and n is number of charge carriers, so its value is decided by the type of host materials and the lithium concentration. [28]

$$V_{open\ circuit\ voltage} = \frac{\Delta G}{nF}$$

Eq. 1

Normally a fully functional series hybrid truck's battery pack requires more than 300 voltage, but a typical lithium-ion battery operates from 3 to 4.2 v. Hence, a multi-cells battery pack, whose cells are connected in series, is utilized in this power-train system. The Lithium Nickel Manganese Cobalt Oxide battery is considered as the most suitable type for this battery pack. It is using the combination of nickel-manganese-cobalt (NMC) as cathode material. The Lithium Nickel Manganese Cobalt Oxide (LiNiMnCoO2) battery has 610–650Wh/kg energy density, 250-340 W/kg specific power, 150–220Wh/kg specific energy. 0.7c–1c charge rate, 1c

discharge rate, around 2000 cycle life, and costs around $450 per kWh. It is apparently the most durable battery with higher energy density from Table 5. [29], which indicates energy density, cost, and lifetime of different types of lithium-ion battery.

Table 5. Cathode materials Overview. [29]

Cathode Material	Energy Density (Wh/kg)	Cost	Lifetime
$LiCoO_2$ (LCO)	546	Medium	Medium
$LiMn_2O_4$ (LMO)	410–492	Low	Low
$LiNiMnCoO_2$ (NMC)	610–650	High	High
$LiFePO_4$ (LFP)	518–587	Medium	High
$LiNiCoAlO_2$ (NCA)	680–760	High	Medium

3.5 Ultra Capacitor

To maximize the recovery of regenerative brake energy, protect battery from rapid charging and discharging overload, and extend battery's life time, a suitable ultracapacitor is set to be used in a high-power situation of this hybrid drivetrain.

First, the type of the capacitor needs to be decided from two storage principles, which are electrochemical double-layer capacitor (EDLC) and electrochemical pseudo-capacitance. Based on Andrew Burke, 'the electrochemical double-layer capacitor (EDLC) is able to store electrostatically energy as positive and negative charges separation in the double layer formed at the interface between the solid electrode material surface [30], which are shown in the electrochemical double-layer capacitor Figure. 18 [31].' It is widely used as the back-up and peak-power sources with battery as the primary sources. [31] By utilizing activated carbon as electrode, the electrochemical double-layer capacitor achieves both higher energy density and higher power density than electrochemical pseudo-capacitance. [30]

28
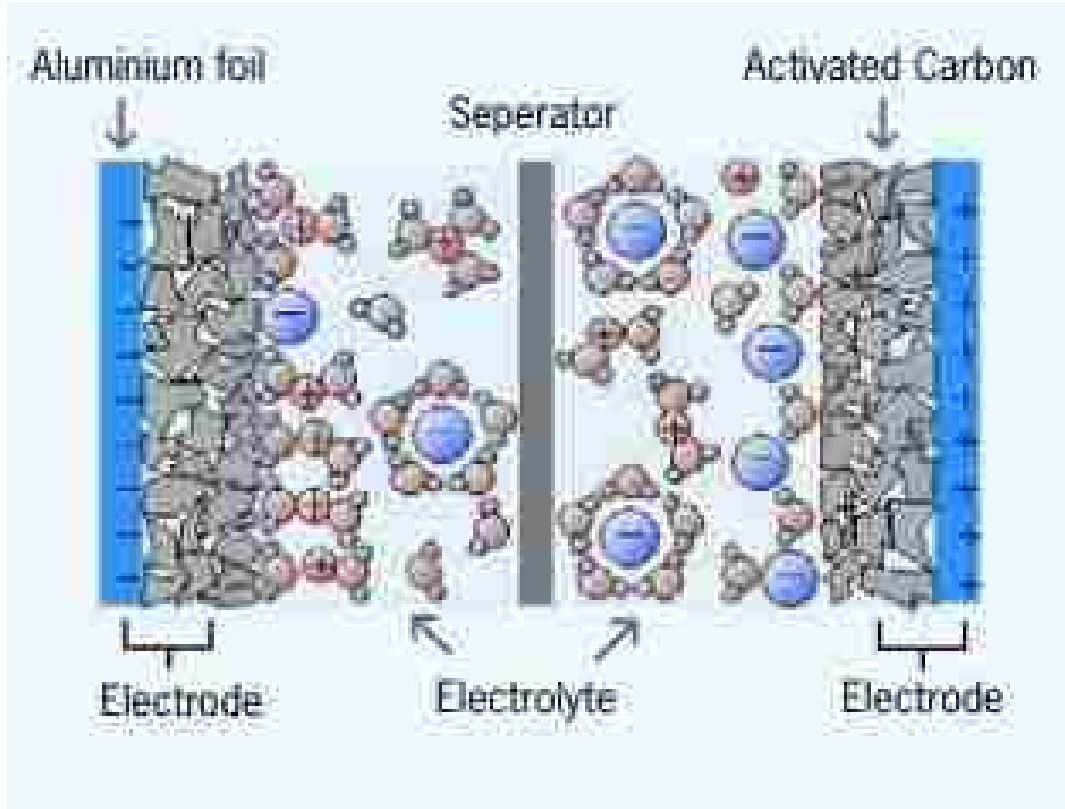
Figure 18. The Electric Double Layer Capacitors (EDLC) Layouts. [31]

Selecting a certain available electrochemical double-layer capacitor (EDLC) on the market depends on the size of the supercapacitor, which is fit to store the maximum regenerative brake energy. The capacitance is the most important characteristic of each ultra-capacitor. The higher equivalent capacitance C_e of the ultra-capacitor, the higher the energy can be stored in it. In Eq. 2, E_c is the energy of super-capacitor, U_{max} is maximum voltage of super-capacitor, U_{min} is minimum allowable voltage of super-capacitor and d is percentage discharge ratio from Eq. 3. [32]

$$C_e = \frac{2E_c}{U_{max}^2[1-(d/100)^2]} \qquad \text{Eq. 2 [32]}$$

$$d = \frac{U_{min}}{U_{max}} \times 100 \qquad \text{Eq. 3 [32]}$$

3.6 Brake Energy Recovery System

In the configuration of the single motor tandem axle module powered hybrid commercial vehicles, the electric motor has an outer rotor connected with rear differential and an inter rotor connected with front differential. Both front and rear differentials are rotationally coupled with the drive shafts of front and rear tandem axles. When the braking action is started, the controller unit which connects directly to the electric motor drops the applied voltage to be less then back electromotive force (back-EMF) voltage (V_b), so the armature torque is reversed with the armature current. Therefore, the speed of the rotor of the electric motor is falling with the drive shaft connected to the wheels, as along as the power is generated by greater EMF. As we known, the battery has limited capacity, which is more likely to be overloaded by the suddenly large amount of recovered energy. In order to extend the battery life and improve the efficacy, the DC current, generated by electromagnetic field, is stored in an ultra-capacitor first. The controller units will dispatch the energy flow from the ultra-capacitor to slowly charge the battery and power the electric motor later. [11]

The braking performance is always a priority consideration when design a braking system. The capability of braking system is defined as the response speed of stopping vehicles and the stability of the vehicles' braking action at any road condition. In order to stop the vehicle as fast as possible, the braking system has to provide enough torque to slow the rotation of each wheel. Meanwhile, this amount of torque is supposed to be controlled by antilock braking system (ABS), which avoids the wheels to be locked to cause uncontrolled skidding. [23] Due to the function of the single motor tandem axle module powered hybrid commercial vehicles, the braking torque by electric motor/generator is easier to be controlled for each tandem axle. However, the torque control for each wheel is still required, hence two brake rotors are introduced to

site each side of the differential mechanisms on each tandem axle. These two rotors are smaller than big disc brakes for heavy duty vehicles, since the tremendous number of loads on the discs are extracted by motor/generator. For this reason, vehicle weight reduction can be achieved as well as lighter unsprang weight. Furthermore, a conventional brake system is applied to the front axle of the trucks. [11]

CHAPTER 4

Theoretical Simulation and Modeling

This chapter explains theoretical modeling of the series hybrid heavy-duty commercial vehicle powertrain powered by motor tandem axle module and dual diesel engine generator module, presents details of AVL Cruise model, and numerical simulations. These models are used for testing the fuel consumption and drivetrain efficiency of this application on city operated driving cycles.

4.1 Vehicle Dynamics

The simulation process starts by determine the propulsion and braking power requirements of the vehicle. By applying the New York city driving cycle into the vehicle dynamic model, the tire rolling resistance force F_{RR}, aerodynamic drag resistance force F_{aero}, road grading (θ) resistance and inertia resistance will be generated to estimate the tractive force and power of city operated heavy-duty commercial vehicles. [12]

4.1.1 Aerodynamic Drag

The aerodynamic drag, also known as fluid resistance, is basically a friction force acting opposite to the body of moving subject from the surrounding air. In vehicle dynamics, it can exist as viscous friction between air and the surfaces of vehicle and shape drag from the high-pressure zone at the front of the vehicle to the low-pressure zone at the tail of the vehicle as Figure 19 showed.
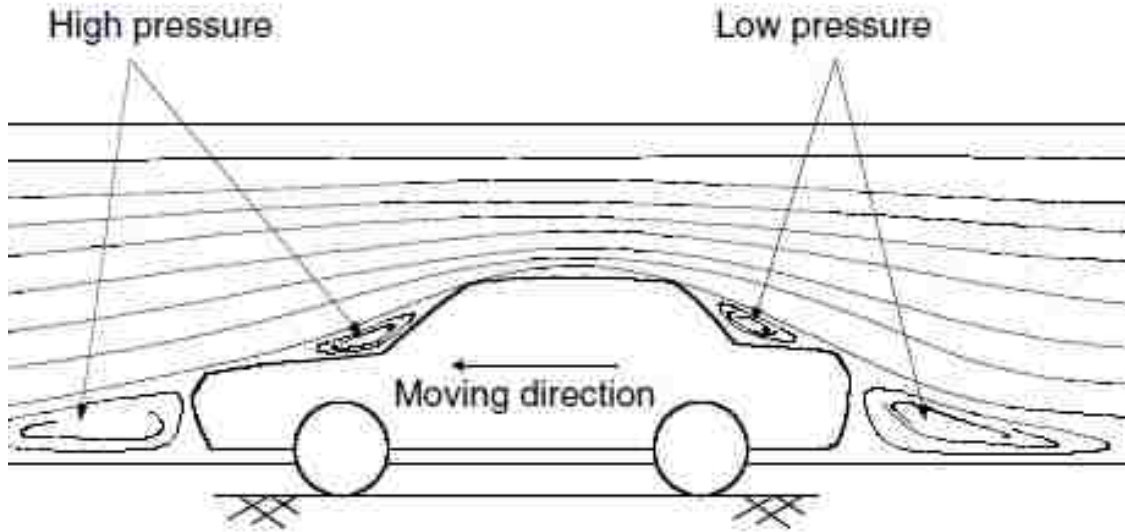
Figure 19. Shape Drag [33]

Hence, aerodynamic drag resistance force F_{aero} can be calculated as Eq. 4, where ρ_{air} is the density of air, C_D is the aerodynamic drag coefficient of vehicle body, A_f is the frontal area of the vehicle, and V_f is the final speed of the vehicle. [27]

$$F_{aero} = \frac{1}{2}\rho_{air}C_D A_f V_f^2 \qquad \text{Eq. 4 [27]}$$

4.1.2 Rolling resistance

Rolling resistance is the force resisting the motion when a subject is rolling on a hard surface, which is caused by the deformation of the rolling subject's material and hard surface. It normally occurs between vehicle wheels and road surface, where the deformation of the tires' material causes hysteresis losses, which results in a distribution of ground reaction forces shifting forward. [27] Thus, a resist rolling moment T_r formed by the forward shifted ground reaction force and normal load as Figure 20. showed.
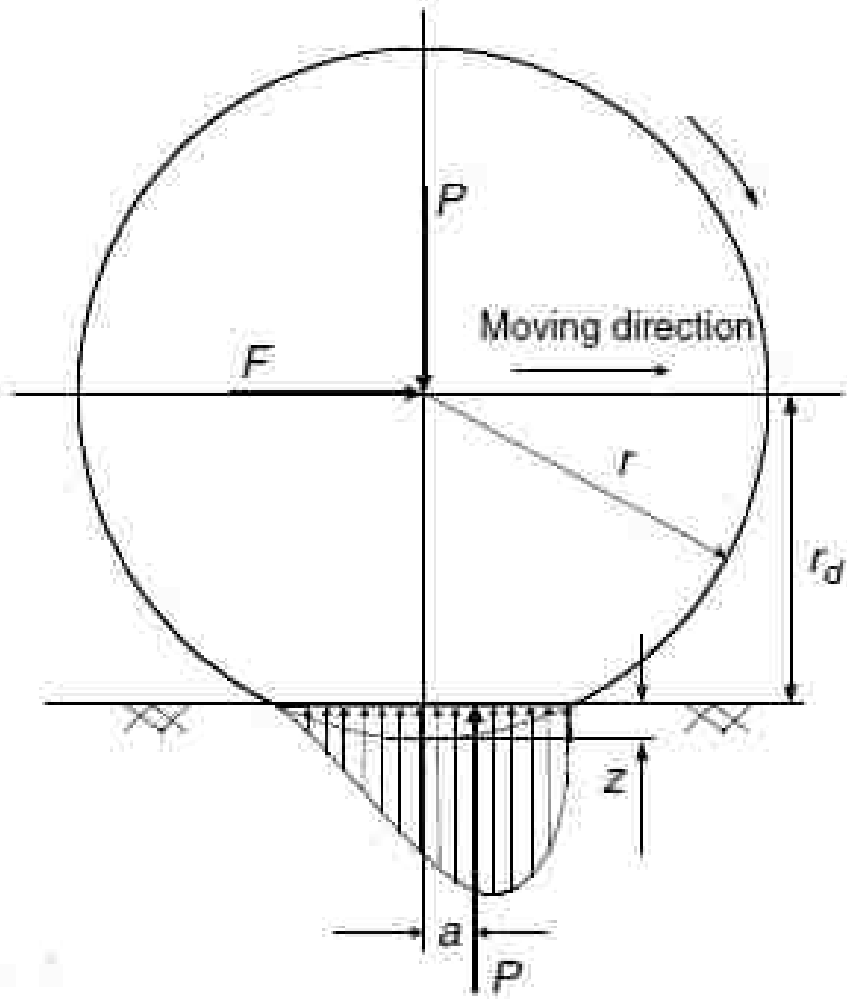
Figure 20. Tire deflection and rolling resistance on a road surface [33]

The rolling resistant moment, as shown in Figure 20. can be calculated by Eq. 5 [33] where P is norm load and a is the shifted distance from center of the tires. The rolling resistance F_r, is the equivalent force opposite to the force F in Figure 20., and can be expressed as Eq. 6 [33]. Considering that vehicles normally travels on surfaces that are not horizontal, a slope θ is applied to Eq. 6 to achieve the final rolling resistance F_{RR} in Eq. 7, where f_r is the rolling resistance coefficient which is ratio of shifted distance from center of the tires a to effective radius of the tire r_d. The rolling resistance coefficient is normally around 0.01 for low-resistance tires on heavy-duty commercial vehicles. [33]

$$T_r = \text{Pa} \qquad\qquad \text{Eq. 5 [33]}$$

$$F_r = \text{F} = \frac{T_r}{r_d} = \frac{Pa}{r_d} = Pf_r \qquad\qquad \text{Eq. 6 [33]}$$

$$F_{RR} = Pf_r cos\theta \qquad\qquad \text{Eq. 7 [33]}$$

4.1.3 Grading resistance

When road has an upward or downward slope, which is more common in real world applications, the vehicle is either experiencing resistance in the uphill trip or assistance in the downhill trip. This resistance or assistance force is called grading resistance F_{GR} that is given by Eq. 8. [33]

$$F_{GR} = \text{mgsin}(\theta) \qquad\qquad \text{Eq. 8 [33]}$$

4.1.4 Inertial resistance

The rotational inertia resistance can be produced by the acceleration of the vehicle and its spinning components. As the Newton's second law of motion stated, the inertia resistance F_{IR} can be expressed as Eq. 9. [27]

$$F_{IR} = m\frac{dv}{dt} \qquad\qquad \text{Eq. 9}$$

4.1.5 Tractive Force and Power

According to the resistive forces diagram for car model on Figure 21., the tractive force F_{trac} must be estimated by Eq. 10 and Eq. 11. [12]
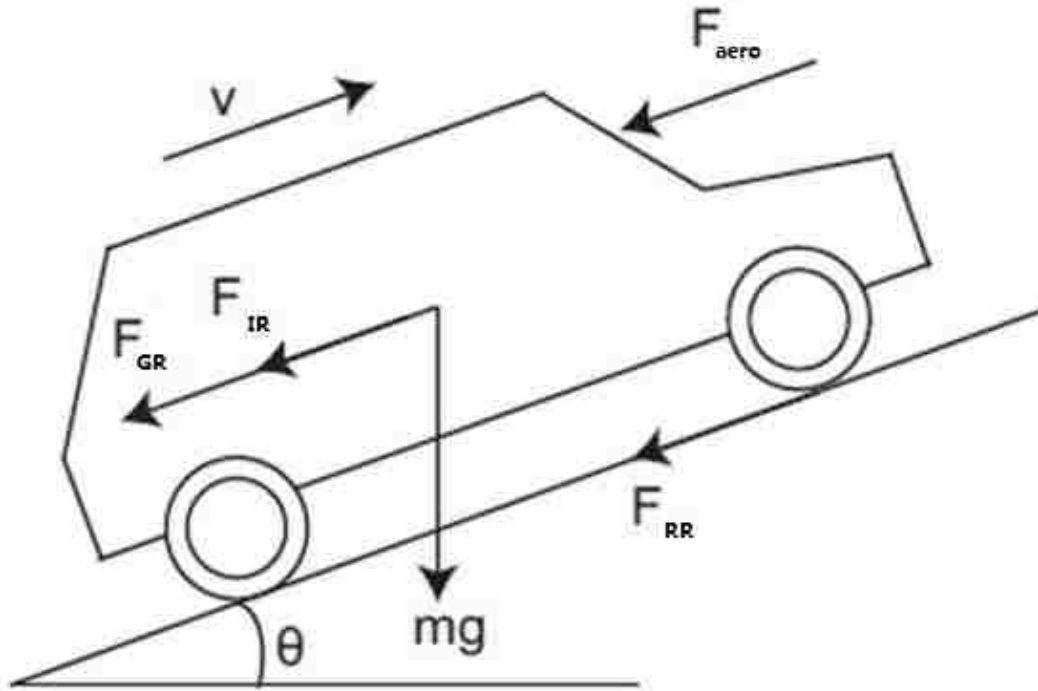
Figure 21. Resistive Forces Diagram for Car Model [27]

$$F_{trac} = F_{IR} + F_{GR} + F_{RR} + F_{aero} \qquad \text{Eq. 10}$$

$$F_{trac} = m\frac{dv}{dt} + mgsin(\theta) + Pf_r cos\theta + \frac{1}{2}\rho_{air}C_D A_f V_f^2 \quad \text{Eq. 11}$$

The curb weight of the vehicle is 23000 Kg, while gross weight m is 25000kg. The dv is the speed difference of the vehicle, g is the gravity acceleration in 9.80 m/s2, θ is the road grading. After multiply Equation 1 by vehicle final speed V_f, the power rating of the motor P_{trac} can be estimated as Equation. 12.

$$P_{trac} = mV_f\frac{dv}{dt} + mgV_f sin(\theta) + \frac{2}{3}mgV_f f_r cos\theta + \frac{1}{5}\rho_{air}gC_D A_f V_f^3 \quad \text{Eq. 12}$$

Where V_f is the final acceleration speed of 105 km/h, as the speed limits for urban commercial vehicles in Toronto, Canada, ρ_{air} is the air density in 1.202 kg/m3, f_r is the tire rolling resistance coefficient assumed as 0.01, A_f is the front area of the

normal rear loading collection vehicle in 10.75m2, and C_D is the aerodynamic drag coefficient assumed to be 0.5. [12] By applying the New York City driving cycle into the vehicle dynamic model in MATLAB, the result is presented in Figure 22. [12], where the required power with no regenerative braking can be reflected as 485kw. Meanwhile, the available power for regenerative braking system is going to be the overall required braking power, which is the same value of 485 kW in different direction, times the estimated 77% regenerative braking efficiency. [12]
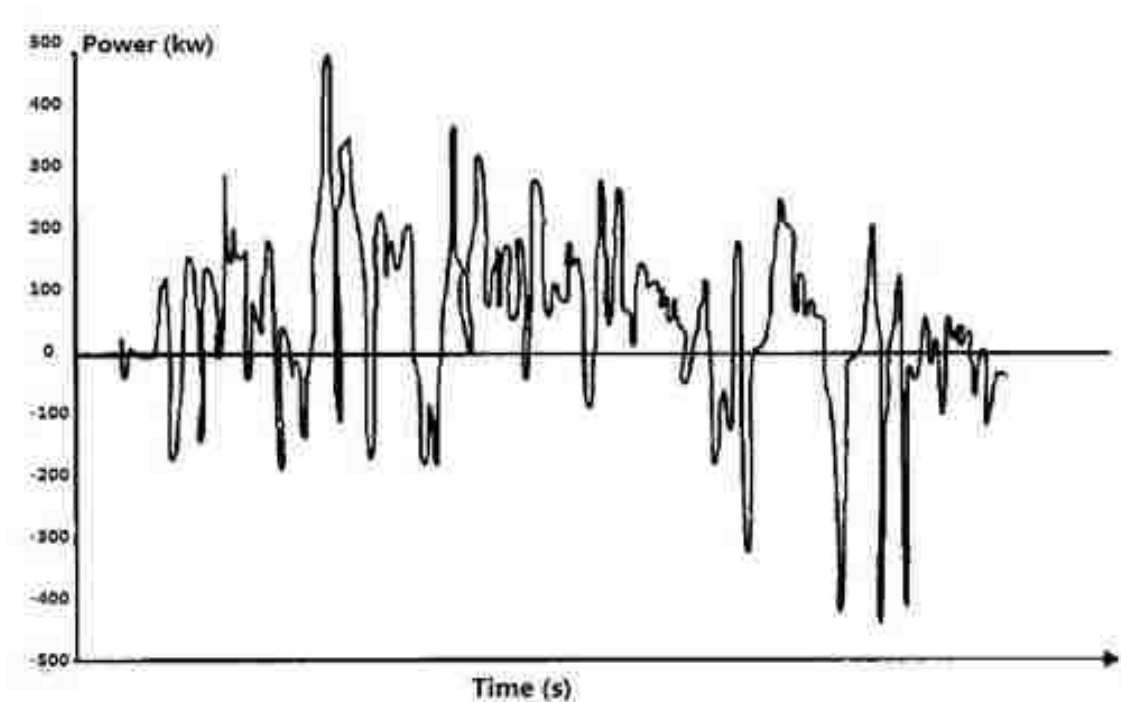
Figure 22. Drive Cycle Power Diagrams by Dynamic Model [12]

4.2 Diesel Engine

The diesel engine in this application is mainly working as the primary power source for the generator. Unlike the conventional diesel engines of heavy trucks, this diesel engine is set to be constantly operated at most optimal engine speed. In this case, the minimum specific fuel economy and most efficient characteristics of the engine with enough power output are required to be determined.

The typical fuel economy characteristic of an internal combustion engine is shown in Figure 23. [34], where the optimal operation area is located within the center area of the oval-shaped contours. When engine operates at the most optimal operation point, which is around 2500 rpm engine speed with 50 kw power output, its minimum specific fuel consumption is at lowest level. Since the engine consumes the least amount of fuel within that area, the engine efficiency also reaches its best at that operating point. Therefore, the lowest fuel consumption for its power output is determined by the load power P_i and the specific fuel consumption g_i, and best efficiency of the engine is determined by power output and fuel energy input. [27] The total fuel consumption of a driving cycle Q_t can be calculated by Eq. 13, where ρ_{fuel} is the mass density of fuel and Δt is the time interval of whole cycle.[33] The engine efficiency, η_e, is obtained by Eq. 14, where T_e is the torque output of engine, ω_e is the output speed of engine, $\dot{Q}_t$ is the rate of fuel consumption, and H_{fuel} is the heating value of the fuel. [27]

$$Q_t = \sum_i \frac{P_i g_i}{1000 \rho_{fuel}} \Delta t \qquad \text{Eq. 13 [33]}$$

$$\eta_e = \frac{T_e \omega_e}{\dot{Q}_t H_{fuel}} \qquad \text{Eq. 14 [27]}$$
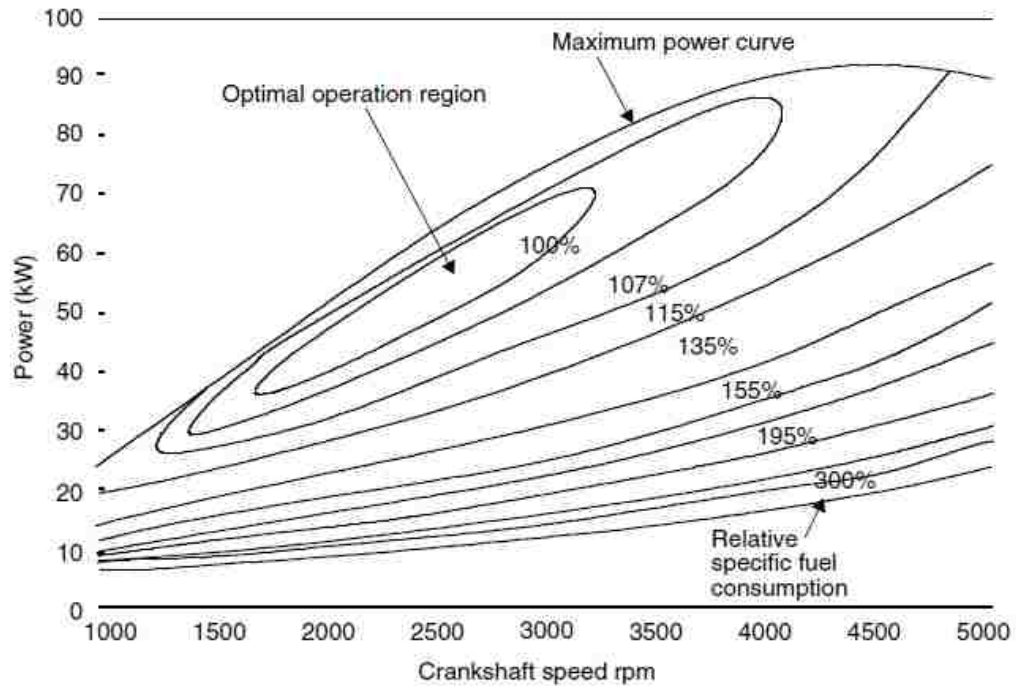
Figure 23. Example of Engine Characteristics and Optimal Operating Region [34]

Based on the results of dynamic model, the eight cylinders turbocharged diesel engines was selected in this application, which has 8478 cm3 displacement and 80 ℃ working temperature. The fuel type is selected as diesel with 44000kJ/kg heating value and 0.76 kg/l density. By entering all the parameters into engine model from the AVL Cruise database, the engine fuel map is generated as Figure 24., where diesel engine reaches its optimal operation point at engine speed of 1000 rpm.
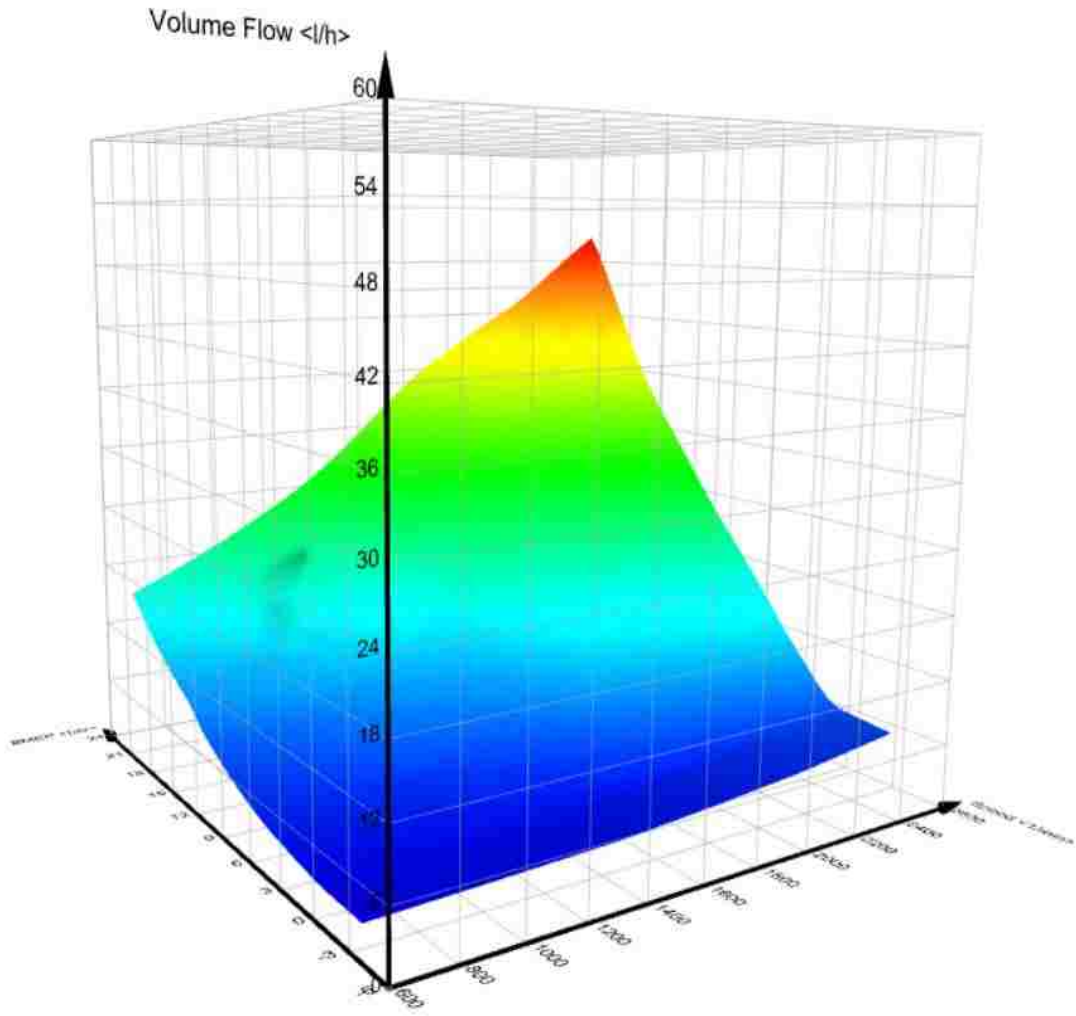
Figure 24. Engine Fuel Map

4.3 Electric Components

4.3.1 Motor and Generator

The efficiency and the maximum torque are the most important properties for both the electric motor and the generator. Since the torque output of the electric motor, T_{out}, is equal to power output P_{out} times efficiency η_{em} divided by angular speed ω, and power rating of the electric motor has been indicated as the required power 485kw in vehicle dynamic model, the efficiency of the electric motor can be calculated with respect to speed and torque. The tractive force, $F_{trac,}$ is applied to the wheels with radius

40

R, which is selected as 515 mm, so the torque on the wheel, T_w, can be calculated as

Eq. 15. The required output torque of motor, T_{out_req}, transfers to the wheels though a

differential on each axle. Hence, the output torque of motor can be obtained by Eq. 16,

where N_{dif} is the differential ratios of 6.06.

$$T_w = F_{trac}R \qquad \text{Eq. 15}$$

$$T_{out\_req} = \frac{2T_w}{N_{dif}} \qquad \text{Eq. 16}$$

After established the estimation, an electric machine model has been created in

AVL Cruise, which is a 360 V nominal voltage motor with 10000 1/min maximum

speed and 2472 Nm maximum torque. It is shown in Figure 25. that motor torque is

constant from zero speed to 3000 1/min, which is called corner speed that limits motor

torque to maximum value.
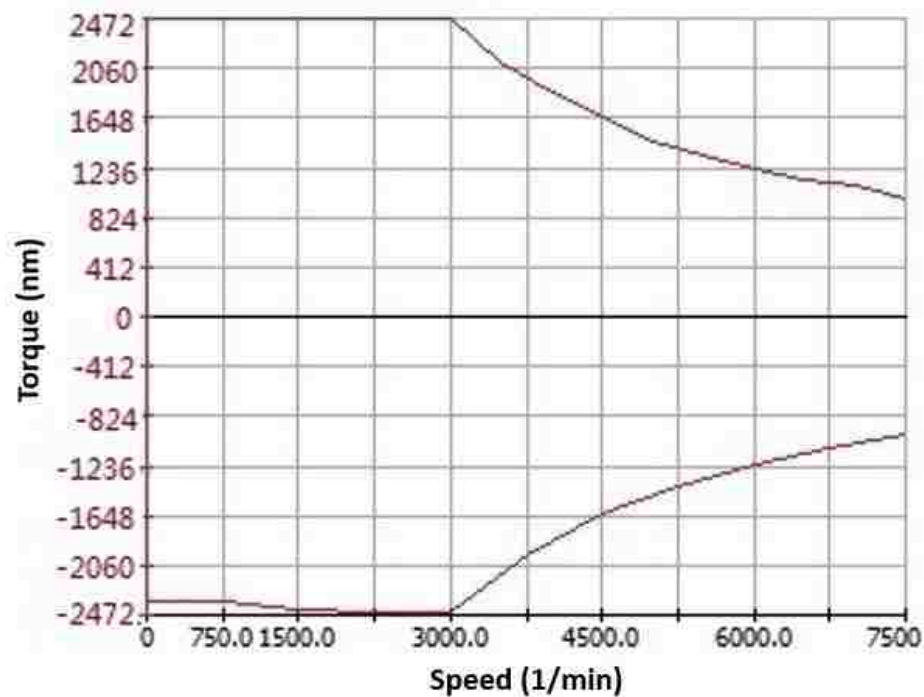
Figure 25. Speed-Torque Curve of Electric Motor

The efficiency of the electric motor is also shown in Figure 26. The highest efficiency of 93% happens when speed reaches around 4900 1/min and torque is around 1300 Nm.
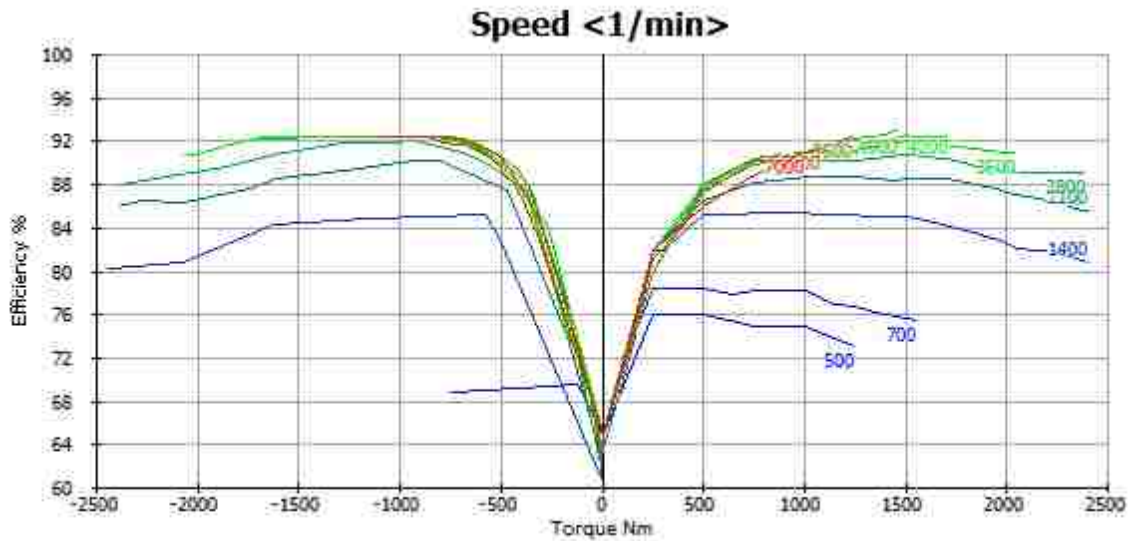
Figure 26. Efficiency Map of Electric Motor

4.3.2 Battery

A multi-cells lithium nickel manganese cobalt oxide (NMC) battery pack is adopted in this application. In order to figure out the size of battery for this drivetrain, the whole battery pack is modelled as a simple resistance model as in Figure 27.
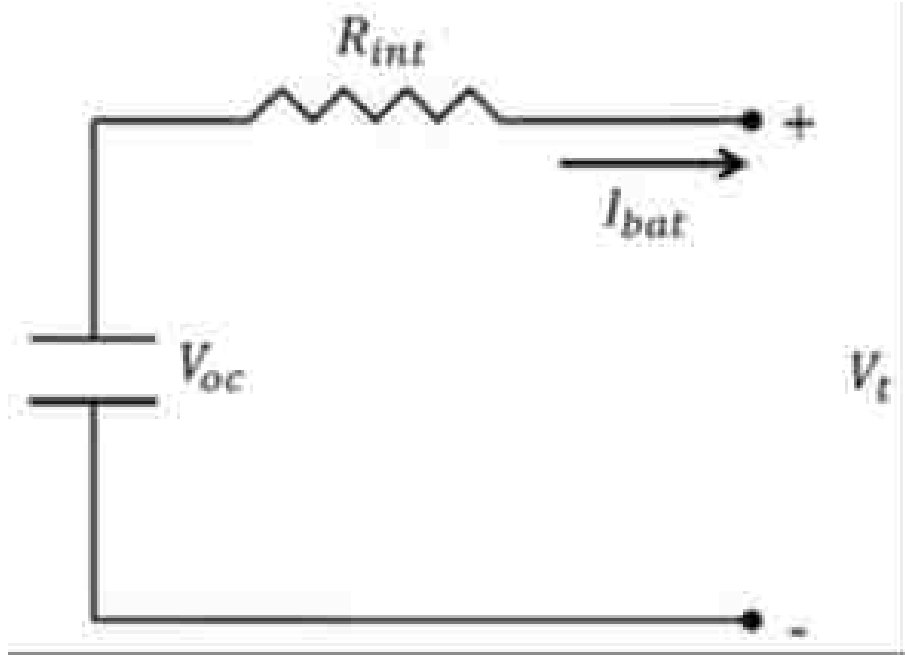
Figure 27. Schematic Model of The Battery Model [21]

The terminal voltage of whole multi-cell, which is the potential difference between the battery terminals with load applied, can be calculated as a simple resistor capacitor circuit in Eq. 17, where V_{oc} is open circuit voltage, R_{int} is internal resistance of the battery, V_t is battery terminal voltage and I_{bat} is battery output current. [12]

$$V_t = V_{oc} - I_{bat}°R_{int}$$

Eq. 17 [21]

The open circuit voltage is the voltage between the battery terminals with no load applied, which is a function of the battery state of charge (SOC). Meanwhile, internal resistance of the battery, which causes decline in efficiency η_{batt} when increasing, is also a function of state of charge (SOC). According to Karin Jonasson, the sum of electric power output of the battery, P_{batt}, is equal to the battery losses that act on the deviation of power, which is the demanded power from drivetrain system, can be expressed as Eq. 18. [35] Thus, the terminal voltage of the whole battery pack

is 360 V, which results in a 100 cells of lithium nickel manganese cobalt oxide (NMC) battery.

$$P_{batt} = V_{oc}I_{bat} \qquad \text{Eq. 18}$$

When power loss from other battery power electric components like air condition and fan is neglected in this model, the battery efficiency, η_{batt}, can be expressed as Eq. 19, when the battery is charged or discharged by power P_{charge}. Therefore, the total battery efficiency is also based on the current state of charge of battery. [35]

$$\eta_{batt} = \frac{P_{charge}}{P_{batt}} \qquad \text{Eq. 19 [35]}$$

4.3.3 Ultra Capacitor

The size of super-capacitor is based on the maximum energy E_{max} demanded to be stored, which basically depends on regenerative braking. According to vehicle dynamics model the regenerative braking system will be able to restore 373kw power during the braking action. The maximum energy storage, E_{max}, can be also be expressed as Eq. 20.

$$E_{max} = \frac{C_e U_{max}^2}{2} \qquad \text{Eq. 20 [32]}$$

The equivalent capacitance, C_e, which can be calculated by Eq. 2., where E_c is the energy of ultracapacitor can provide, U_{max} is maximum voltage of ultracapacitor, U_{min} is minimum allowable voltage of ultracapacitor and d is percentage discharge ratio from Eq. 3. The energy releases from ultracapacitor bank is presented as Eq. 21, and maximum power, P_{max}, the ultracapacitor can provide is presented in Eq. 22, where R_e is equivalent series resistance of ultracapacitor.

$$E_u = \frac{C_e(U_{max}-U_{min})^2}{2} \qquad \text{Eq. 21}$$

$$P_{max} = \frac{U_{max}^2}{4R_e} \qquad \text{Eq. 22}$$

As most available electrochemical double-layer ultracapacitors (EDLC) on markets demonstrated, ultracapacitors can be connected in series and parallel and work as a multi-cell ultracapacitor bank. Thus, the equivalent capacitance of each cell times number of series connected cells divided by number of parallel connected cells can result in the equivalent capacitance C_e. For this application the equivalent capacitance of each cell is 100 Farad, nominal voltage of each cell is 36 V, and total 10 cells connected in series.

4.4 Control Strategies

The on-board controller consists of three function modules, which are electric brake and mechanical brake unit, electric drive control unite, and range extender control unit. These units are working as written control-code developed by the control strategies. The maximum state-of-charge of peaking power source control strategy has been developed in this application, since engine can be turned off when SOC of battery reaches a certain level or operates at its most optimized engine speed for better efficiency. Based on Dr. Oriet's design analysis of dual diesel engine generator, there is sufficient power and torque to propel most heavy duty trucks on high way from only one engine, hence the controller can shut down one of the dual engines during the drive cycle requiring less power. When the truck vehicle is accelerating or experiencing high demand driving cycle, the controller brings the second engine back to provide the additional power required, so the efficiency of the generator is significantly improved by optimized variable power delivery. [25] Meanwhile, both of engines can be

continuously runs at the optimized engine speed to drive the generator charging the battery, when SOC of the battery is less than 30%. When SOC of the battery reaches 80% of its maximum capacity, the generator will be turned off by controller, so enough capacity can be reserved for regenerative braking energy. Eq. 21 can be used to indicate the SOC for the battery, where SOC_i is initial state of charge, A is amp-hour, and t is time[21].

$$SOC = SOC_i - \frac{\int_0^t I_{bat} dt}{A} \qquad \text{Eq. 23}$$

This control strategy is also suitable for the vehicles with frequent stop–go driving cycles.[33] When the braking action starts, the controller unit will turn the motor into a generator, so the back electromotive force voltage became greater then applied voltage, which will change the direction of the armature current. The reversed armature torque is provided to stop the vehicle from moving, and the braking energy can be recovered as electric power. The mechanical brake and anti-braking system will also be brought in action per the magnitude of requested braking power and wheel motions. [12]

CHAPTER 5

Simulation Result Analysis

In this chapter, the details of simulation experiments for both conventional heavy-duty commercial trucks and the electric tandem axle module powered series hybrid commercial truck are presented. The set-up and drive cycles are included in this chapter along with the simulation result, which mainly focused on the comparisons of drivetrain efficiency and fuel consumption.

5.1 Simulation Set-up

The simulation tool for this thesis is AVL Cruise, a preprogramed software assists in vehicle driveline system analysis that includes all the applications needed in this thesis like fuel efficiency, driving emissions and performance analyses. According to Figure 28. from the AVL CRUISE training course, it is recommended to initiate the project by creating vehicle model, imputing data generated from Chapter 4 into components, and establishing energetic connections.
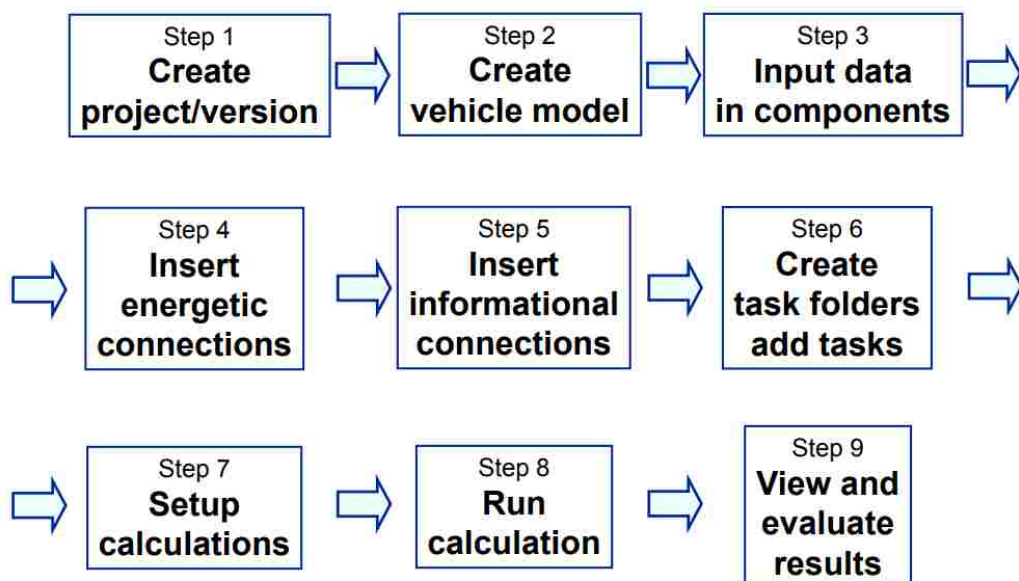

Figure 28. Recommended Work Process Flow [36]

Frist of all, a conventional heavy-duty commercial vehicle model is created in AVL Cruise as Figure 29. demonstrated. The property inputs of the truck vehicle setting like gas tank volume, vehicle body dimensions, load dependent characteristics, curb weight, and air coefficient are identical to the new series hybrid truck. The 8-cylinder turbocharged intercool diesel engine has 8478 cm3 displacement and 80 ℃ working temperature. The fuel type selected as diesel with 44000kJ/kg heating value and 0.76 kg/l density. The blue lines represent mechanical energetic connection transfer torque from the engine through a friction clutch, an 8-speed gear box, and a differential to wheels on rear tandem axles.
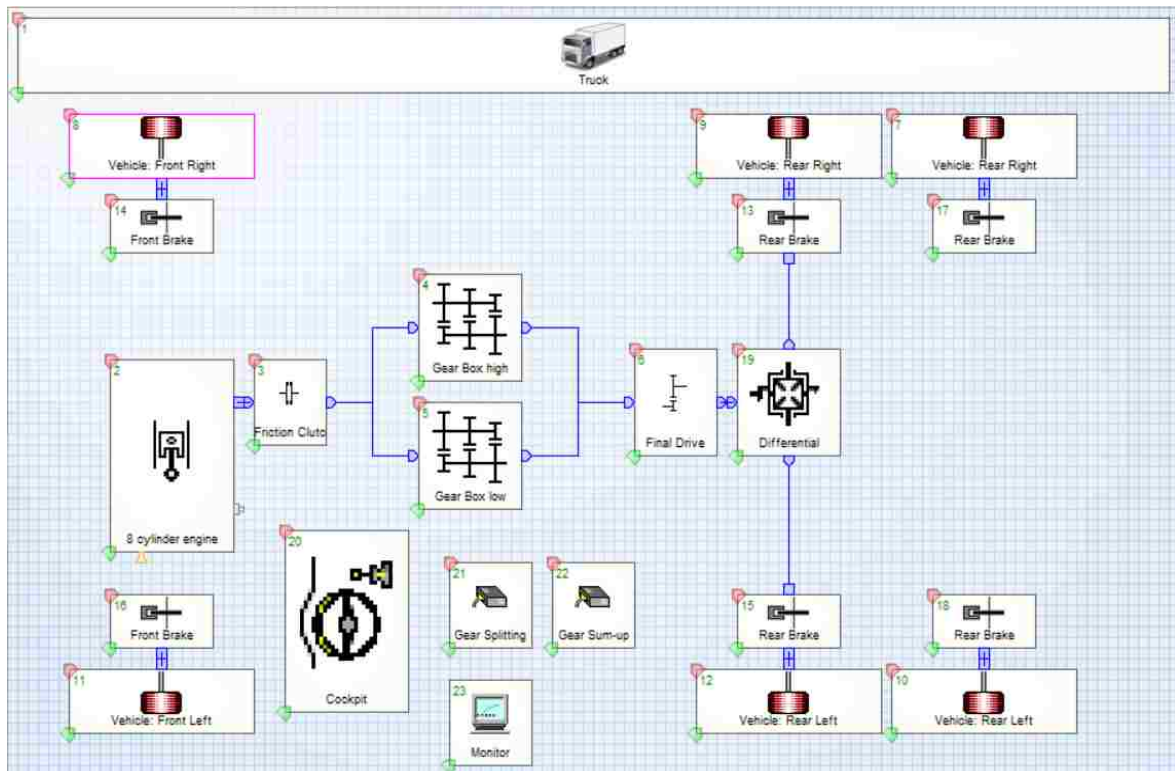

Figure 29. Conventional Heavy-Duty Commercial Vehicle Model

The model of the electric tandem axle module powered series hybrid commercial vehicles is also shown in Figure 30., where red lines are electrical connections and blue lines are mechanical connections. The data of diesel engine,

48

battery, supercapacitor, electric motor, and generator gathered from theoretical calculations has been put into each component. The acceleration pedal and brake pedal data has been imported into the cockpit, which is the modules that links the driver and the vehicle, the available information of possible to influence the vehicle can be defined by using the monitor set up. The load signal from cockpit, velocity of vehicle, torque of electric drive, SOC of the battery, and engine speed are added as the input channels into the monitor that can be connected to output channels of different modules to show the output values after running the calculation of the model. [12]
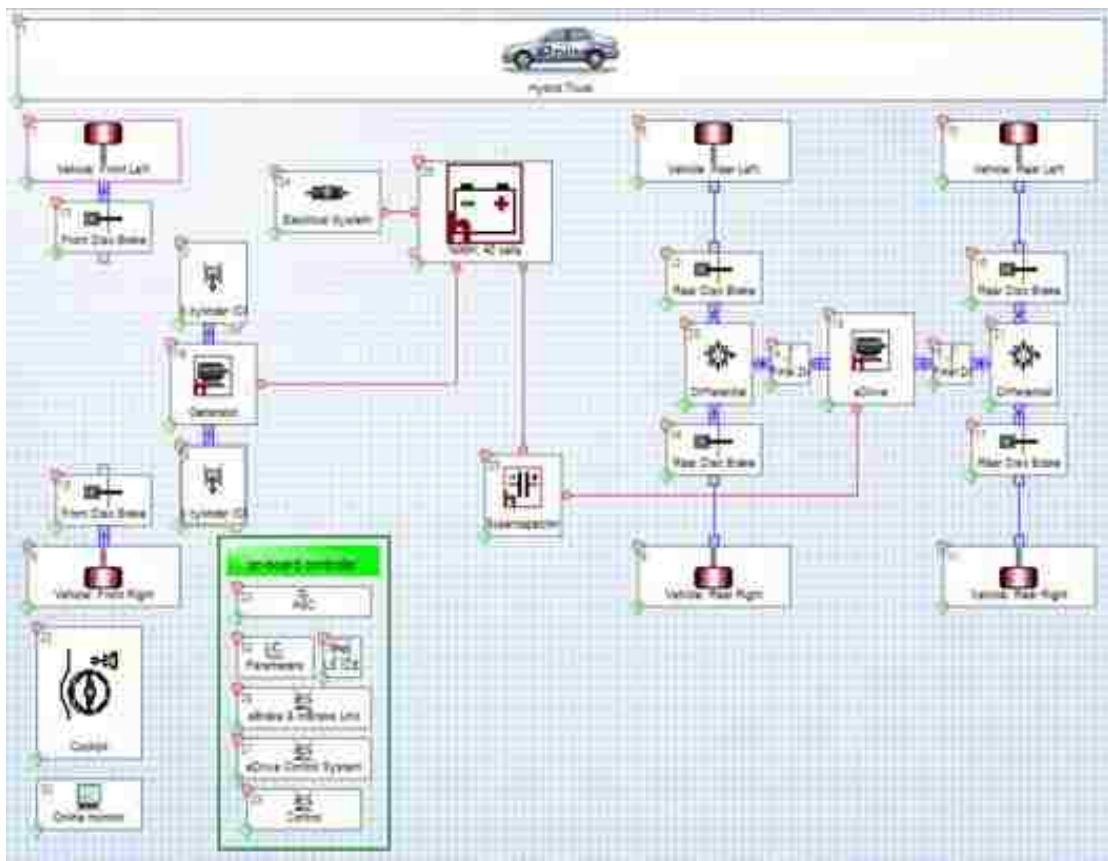

Figure 30. Electric Tandem Axle Module Powered Series Hybrid Commercial Vehicles Model

The final step before setting up the drive cycle for the simulation task is creating the informational connections on the Databus, which are represented as rainbow lines

in Figure 31. The load signal is delivered though the Databus from the engine to the control system, which is modeled as a control function in AVL Cruise model.
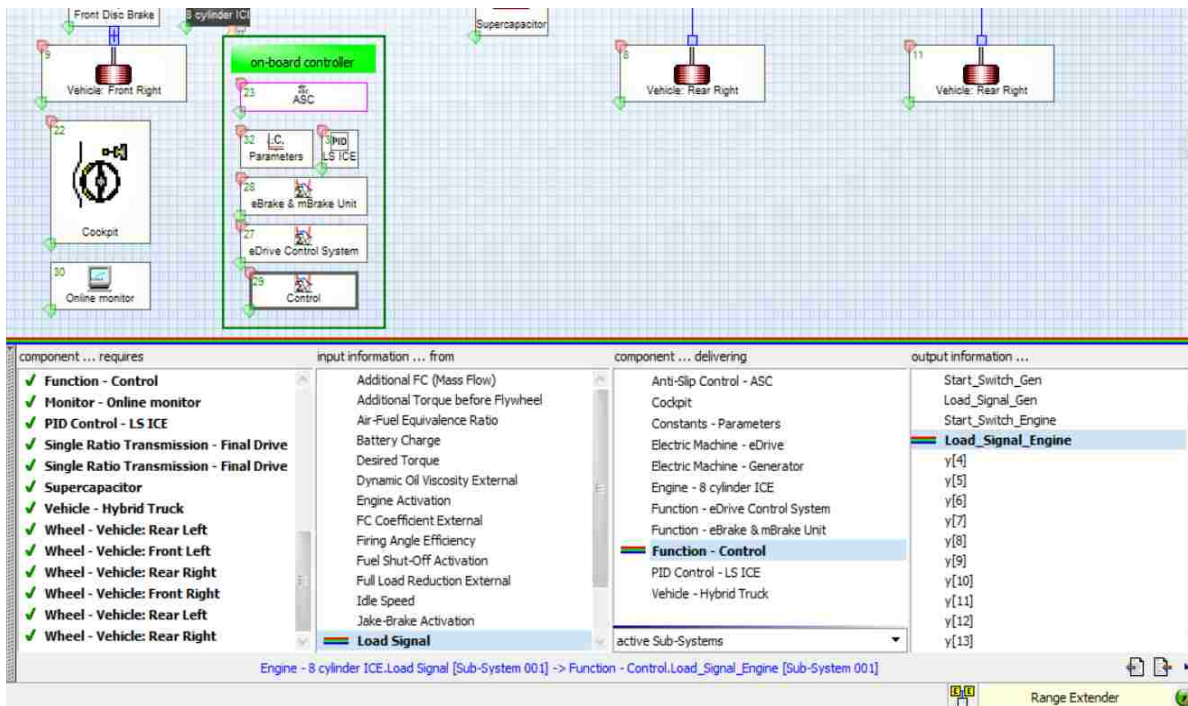
Figure 31. Databus Connections

5.2 Drive Cycles

Using drive cycles to estimate and compare fuel efficiency of two types of trucks is the main goal of simulation process. For this reason, two drive cycles for both city operated and high way operated have been selected from AVL Cruise database. The Figure 32. presents the velocity and distance verse time curves of the city operated drive cycle that is 13.14km long. This cycle has an average speed of 40 km/h, maximum speed of 82 km/h, and 600 s break time.

Figure 32. Velocity and Distance Verse Time Curves of City Operated Drive Cycle

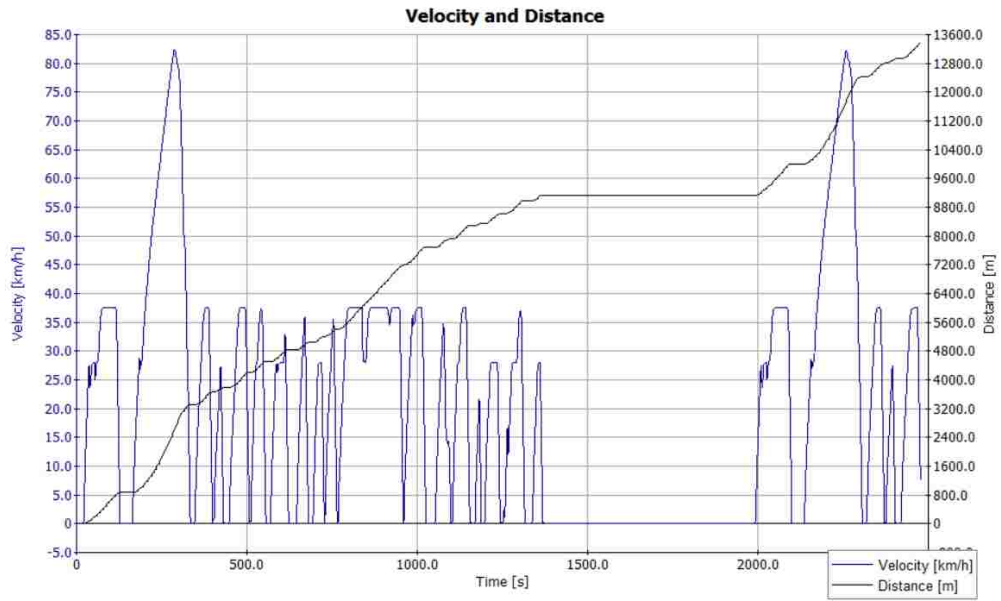For high way operated drive cycle's, the velocity and distance verse time curves in Figure 33., the total distance is 12.1 km. This mean speed is around 80 km/h, maximum speed is 97 km/h, and break time is 80 s at end of the cycle.
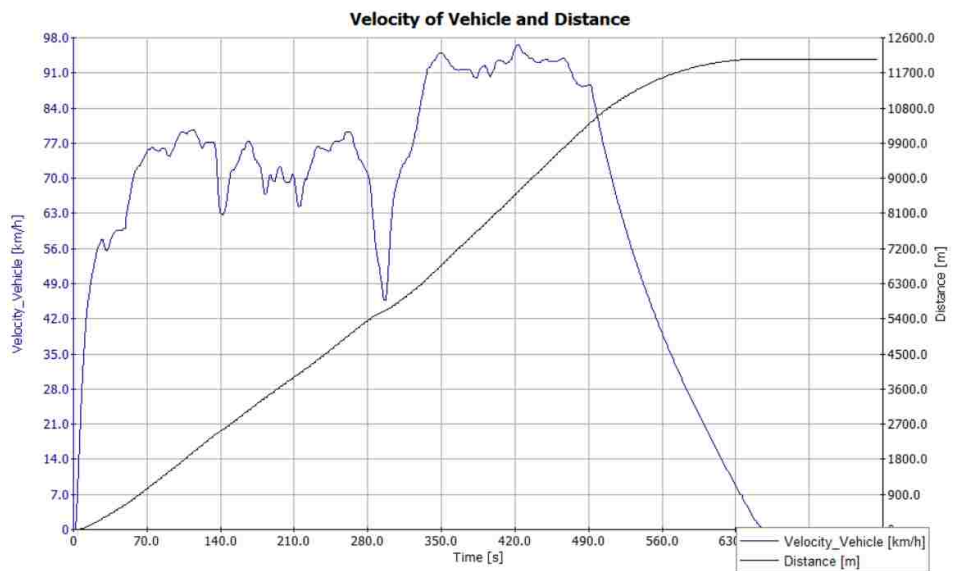

Figure 33. Velocity and Distance Verse Time Curves of Highway Operated Drive

Cycle

By applying these two driving cycles for AVL Cruise Models, the simulation was run under the variable step solver implicit euler+. The results of simulation are generated as time dependent with a standard driver.

5.3 Result Analysis

5.3.1 E-Drive Efficiency

The main improvement of this application when compares to conventional hybrid powertrain system is electrical tandem axle power module with regenerative braking. Therefore, with the optimization of the hybrid electric drivetrain, the efficiency of electric drive should be significantly improved in this application when the city operated drive cycle applied. The plot of electric drive efficiency versus time is given as Fig. 34 evidently states a maximum efficiency of 92%, which is much better than most conventional hybrid trucks' 75%. [12]
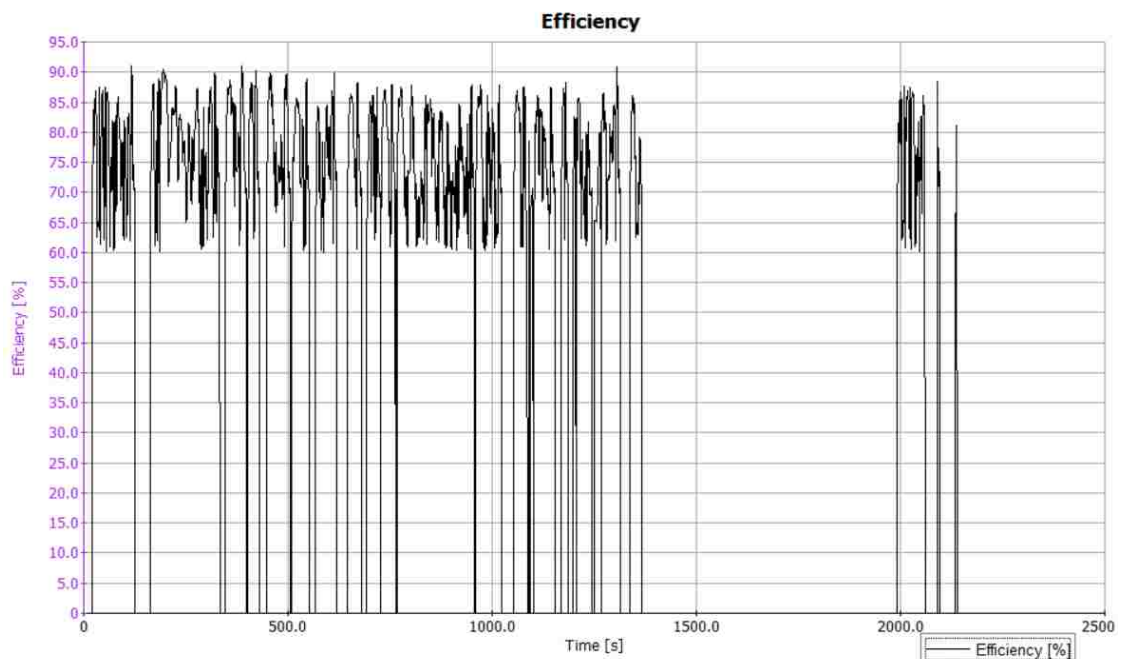

Figure 34. E-Drive Efficiency for City Operated Drive Cycle

When it comes to high way operated drive cycle, the maximum efficiency of the electrical drive is also improved to same level of the city operated condition, as Figure 35. showed.
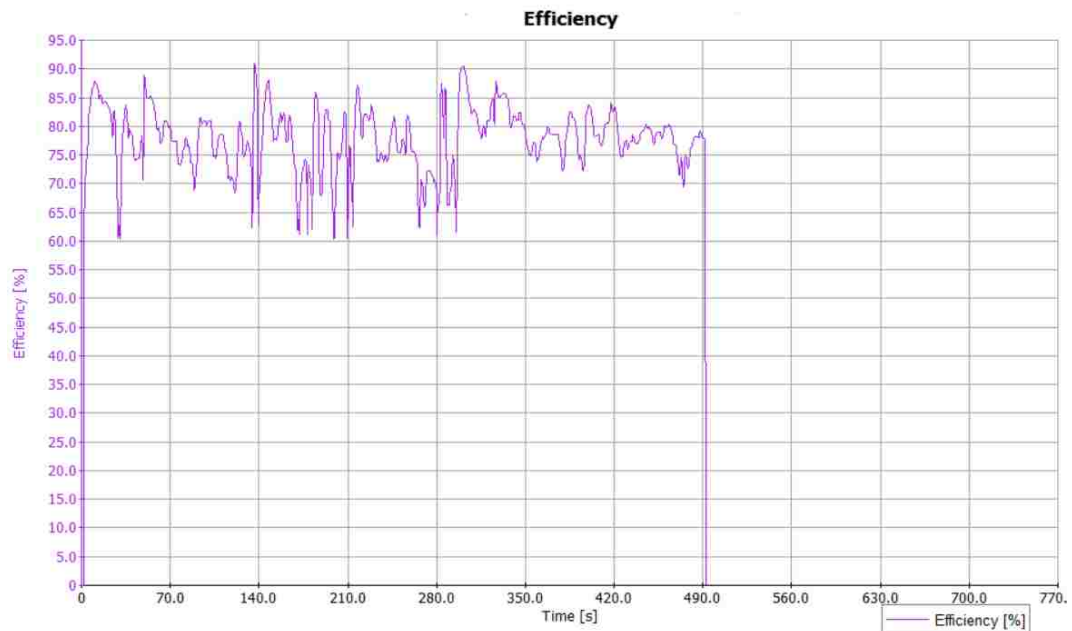
Figure 35. E-Drive Efficiency for High way Operated Drive Cycle

According to the diesel engines efficiency data in AVL Cruise models, the diesel engine can averagely convert over 47% of the fuel energy into mechanical energy. Hence, the average efficiency of whole drivetrain from fuel is around 44% for this new series hybrid drivetrain, and the average efficiency of whole drivetrain from fuel is around 35% for this conventional series hybrid drivetrain.

5.3.2 Fuel Consumption

The electrical hybrid powertrain has optimal engine operation and regenerative braking to improve the efficiency of conventional heavy-duty vehicles. Generally, the more efficient driveline certainly means better fuel economy, and this application is also not exceptional. As Figure 36. recorded, the new hybrid truck consumes 3.4-liter

diesel fuel when drives in a city operated driving cycle and reaches maximum fuel consumption rate of 22 litter per hour only at engine start.
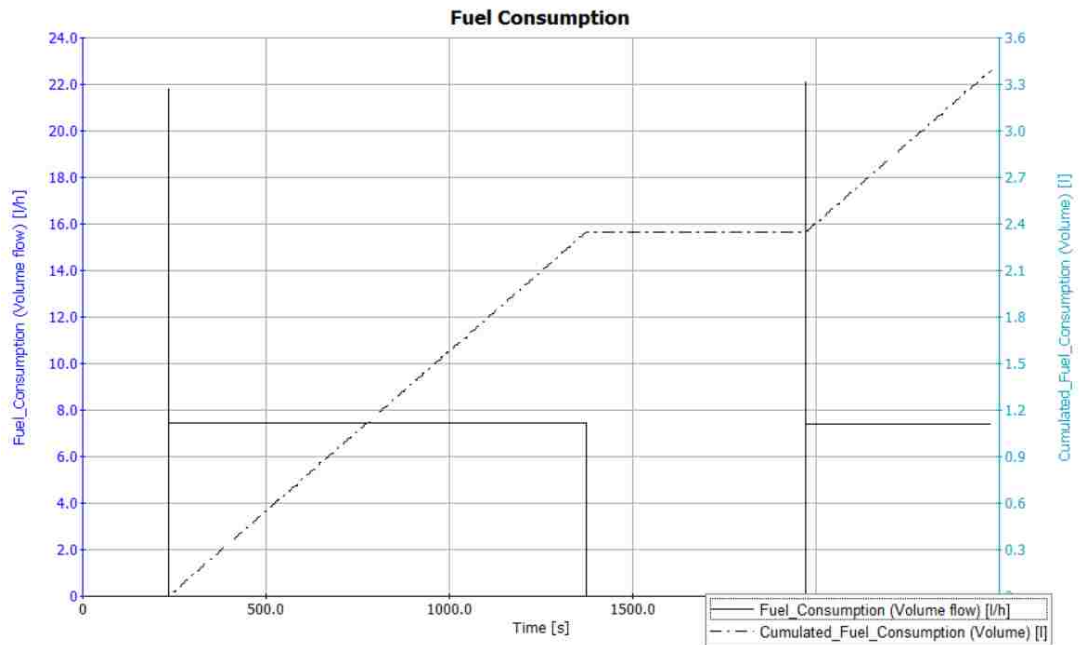
Figure 36. Fuel Consumption of New Hybrid Heavy-Duty Commercial Vehicle for City Operated Driving Cycle

In Figure 37., the conventional heavy-duty commercial vehicle consumes 8.4-liter diesel fuel and constantly reaches a maximum fuel consumption rate of 45 liter per hrs.
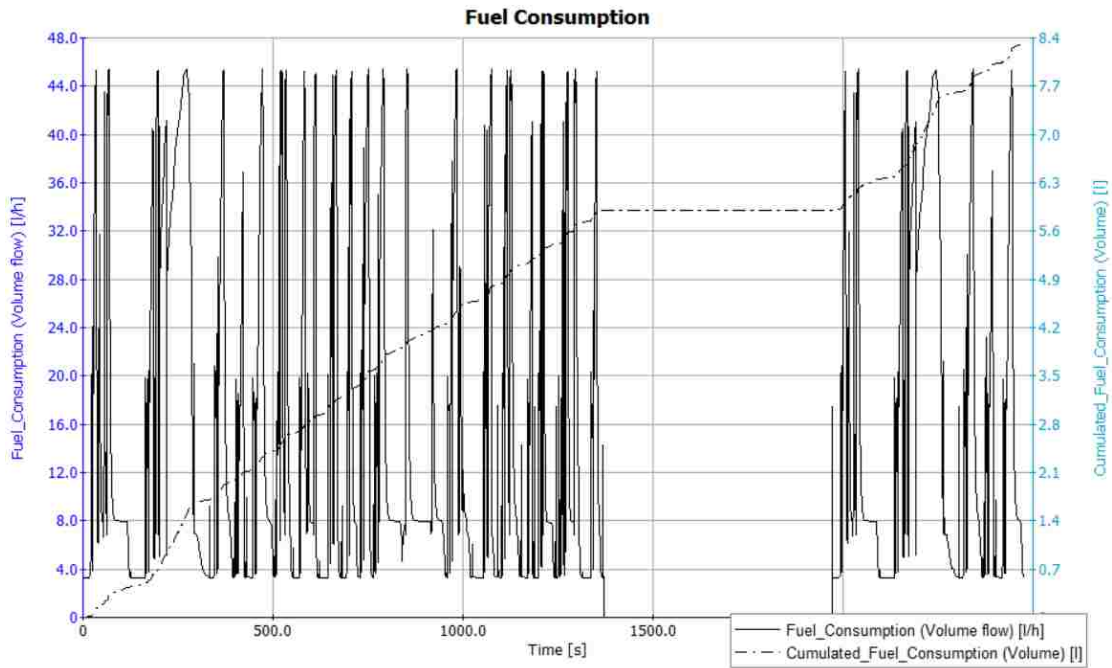
Figure 37. Fuel Consumption of Conventional Heavy-Duty Commercial Vehicle for

City Operated Driving Cycle

Based on the result files from AVL Cruise, the average fuel consumption of the new hybrid heavy-duty commercial vehicle for this driving cycle is 25.81 liters per hundred kilometers. Compare to conventional heavy-duty commercial truck's 62.3 liters per hundred kilometers, the progress of this application's fuel saving is conspicuously in city.
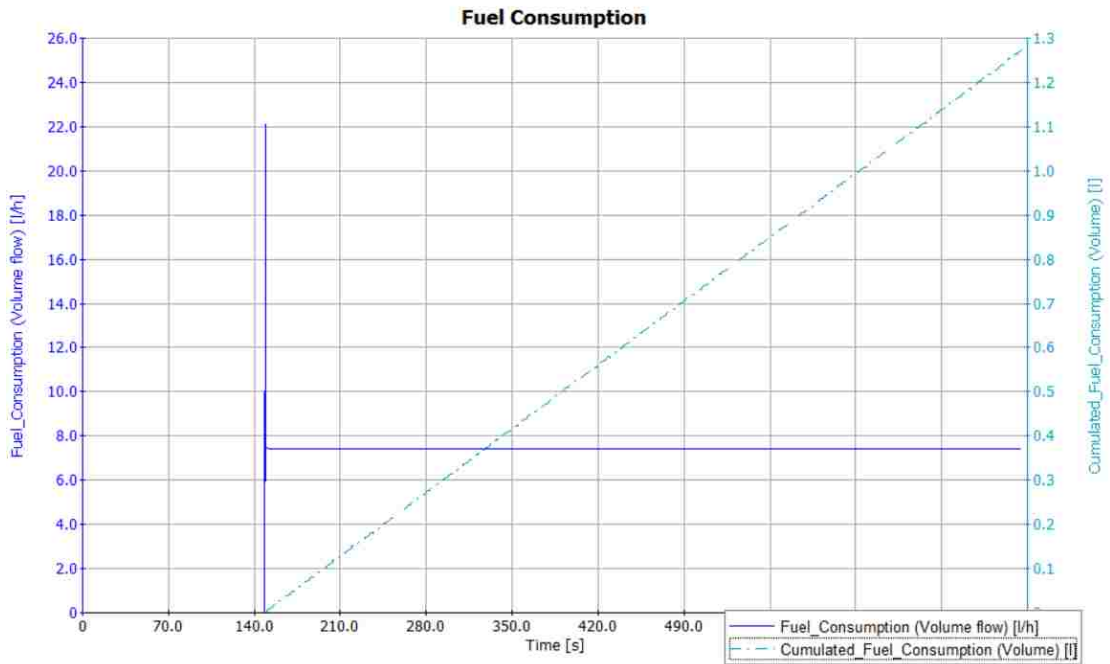
Figure 38. Fuel Consumption of New Hybrid Heavy-Duty Commercial Vehicle for

Highway Operated Driving Cycle

When two vehicles drive on high way operated drive cycle, both of the fuel consumption dropped significantly due to the less decelerations and accelerations. For 12.1 kms, new hybrid heavy-duty commercial vehicle consumes 1.3-liter fuel in Figure 38., and conventional heavy-duty commercial vehicle consume near 3 times fuel of 3.7-liter shown in Figure 39.

Figure 39. Fuel Consumption of Conventional Heavy-Duty Commercial Vehicle for

Highway Operated Driving Cycle

The average fuel consumption of the new hybrid heavy-duty commercial vehicle for the highway drive cycle is 10.55 liters per hundred kilometers, and the conventional heavy-duty commercial truck is 24.8 liters per hundred kilometers, the progress of this application's fuel saving is conspicuously in the city.
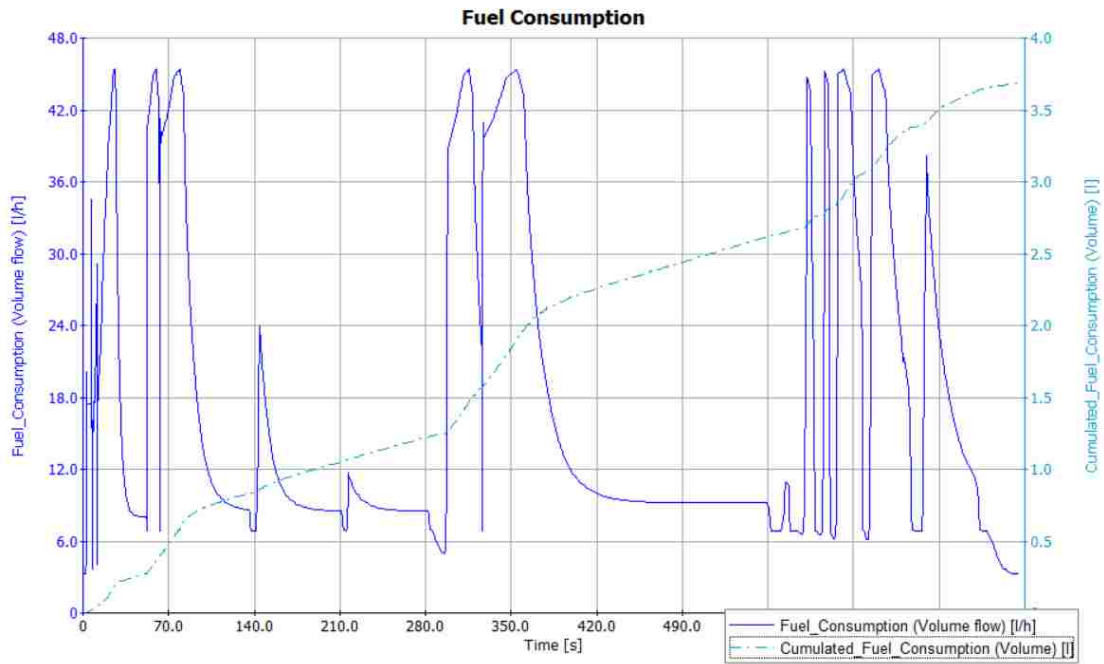
CHAPTER 6

Conclusions

This Thesis demonstrated the design and modeling methodology for the specification of system architectures and hybrid drivetrain control strategies of series hybrid heavy-duty commercial vehicles powered by motor tandem axle module. The simulation methods and results proved the theoretical efficiency and practicability of this application, which has better drivetrain efficiency and fuel economy then convectional hybrid heavy-duty commercial vehicles and conventional heavy-duty commercial vehicles. However, certain loopholes still exist in this simulation approach. Due to the characteristic of dual diesel engine and control strategies of the drivetrain system, two diesel engines barely work together at high power required situation like climbing. The profile of the drive cycle we used does not consider any grading or cornering, so the simulation result might be discrepant to real world test result. Moreover, the optimum modeling of the electrical motor of this application in AVL Cruise or other simulation software could be done in future developments. [12]

REFERENCES/BIBLIOGRAPHY

1. Winston Harrington, Virginia McConnell, "Motor Vehicles and the Environment," Resources for The Future, Washington, D.C, 2003.

2. David Mage, Olivier Zali, "Motor Vehicle Air Pollution Public Health Impact and Control Measure," World Health Organization and ECOTOX, Geneva, Switzerland, 1992.

3. U.S. Environmental Protection Agency, "Inventory of U.S. Greenhouse Gas Emissions and Sinks 1990–2015", EPA 430-P-17-00, 2017.

4. Hansen, J., R. Ruedy, M. Sato, and K. Lo, "Global Surface Temperature Change". Rev. Geophys., 2010, 48, RG4004, doi:10.1029/2010RG000345.

5. Kajsa Lindqvist, "Emission Standards for Light And Heavy Road Vehicles", AirClim Factsheet Number 25, Air Pollution & Climate Secretariat, Göteborg, Sweden, 2012

6. Josh Miller, Li Du, Drew Kodjak, "Impacts of World-Class Vehicle Efficiency and Emissions Regulations in Select G20 Countries", The International Council on Clean Transportation, G20 Regulations Impact Analysis, Washington DC, 2017

7. U.S. Environmental Protection Agency, National Emissions Inventory Air Pollutant Emissions Trends Data, 1970-2013, Average Annual Emissions All Criteria Pollutants, Available at http://www.epa.gov/ttn/chief/trends/index.html (link is external) as of October 2014.

8. Gurdas Sandhu, H. Christopher Frey, Shannon Bartelt-Hunt, Elizabeth Jones, "Real-World Activity and Fuel Use of Diesel and CNG Refuse Trucks," Presentation at PEMS International Conference & Workshop, April. 2014.

9. David L. Greene, "Transitions to Alternative Vehicles and Fuels Report of the NRC Committee," Hydrogen and Fuel Cell Technical Advisory Committee, The National Academies Press, Washington, D.C April. 2013.

10. U.S. Energy Information Administration, "Annual Energy Outlook 2016 Reference case", International Energy Outlook 2016

11. Z. Tang, D. Bhovsar, Y. Zhang, L. Oriet, And E. Lang, "The Development of Regenerative Braking System for Motor Tandem Axle Module in Series Hybrid Commercial Vehicles," Acta Mechanica Et Movilitatem, 2017, ISSN 2525-9350.

12. Z. Tang, L. Oriet, E. Lang, And Y. Zhang, "Modeling, Control, And Simulation Methods for Series Hybrid Heavy-Duty Commercial Vehicles Powered By Motor Tandem Axle Module," IEEE Transportation and Electrification Conference and Expo (ITEC), 2017, ISBN: 978-1-5090-3904-3.

13. Rachel M. Zoyhofski, "Estimates of Emissions from Heavy Duty Diesel Vehicles (HDDV) and Control Strategies Related to Transport Activities Supporting High Volume Hydraulic Fracturing Wells in the Marcellus Shale Formation," Rochester Institute of Technology Rochester, NY, 2016

14. Cummins Engines, "X15 Performance Series for Fire & Emergency (2017) Specifications", https://cumminsengines.com/x15-performance-fire emergency-vehicles?#specifications, 2017

15. Cezary Misiopecki, "Investigation of fuel cell technology for long-haul trucks," The School for Renewable Energy Science in affiliation with University of Iceland, University of Akureyri & SAMME, RMIT University, Akureyri, 2011.

16. Tata Prima, "Prima LX 4923.S Drivetrain", http://in.tataprima.com/trailers/4923s/images/prima-image-drivetrain.jpg, 2017

17. Andrew Norman, John A. Corinchock, Sean Bennett, "Heavy-duty Truck Systems," Delmar Thomson Learning, 2000, ISBN 1435483839

18. MAN Truck & Bus (S.A.) Pty Ltd, "CLA 26280 6x4 BB Tipper", https://www.truck.man.eu/man/media/content_medien/doc/business_websites _south_africa/broschuere/CLA_26280_6x4_BB_Tipper.pdf, South Africa, 2014

19. Sunil Adhikari, "Real-time Power Management of Parallel Full Hybrid Electric Vehicles," Department of Mechanical Engineering, The University of Melbourne, Australia, October, 2010.

20. Karin Jonasson, "Analysing Hybrid Drive System Topologies," Department of Industrial Electrical Engineering and Automation, Lund University, Sweden, 2002.

21. D. Bhovsar, Z. Tang, Y. Zhang, L. Oriet, And E. Lang, "Methodology and Initial Analysis to Compare Hydraulic Hybrid and Electric Hybrid for Commercial Vehicles," Acta Mechanica Et Movilitatem, 2017, ISSN 2525-9350.

22. Nathan C. Nantais. "Active Brake Proportioning and Its Effects on Safety and Performance". University of Windsor: Faculty of Mechanical Engineering Graduate Studies and Research, 2006.

23. Erlston, L. and Miles, M., "Retrofittable Regenerative Braking in Heavy Vehicle Applications," SAE Technical Paper 2008-01-2558, 2008, doi:10.4271/2008-01-2558.

24. U.S. Environmental Protection Agency, "How Series Hydraulic Hybrid Vehicles Work", Office of Transportation and Air Quality (OTAQ), https://archive.epa.gov/otaq/technology/web/html/how-it-works.html.

25. Leo P. Oriet, "Series Hybrid Generator," U.S. Patent No. 20150008055 A1. Jan 8, 2015.

26. Leo P. Oriet, "Structural electric tandem axle module," U.S. Patent No. 0090505. Apr. 2, 2015.

27. Sunil Adhikari. "Real-time Power Management of Parallel Full Hybrid Electric Vehicles". The University of Melbourne: Department of Mechanical Engineering, 2010.

28. Vishal Mahajan. "Fundamentals of lithium-ion electrochemistry". IEEE Transportation and Electrification Conference and Expo (ITEC), 2017.

29. Gert Berckmans, Maarten Messagie, Jelle Smekens, Noshin Omar, Lieselot Vanhaverbeke and Joeri Van Mierlo., " Cost Projection of State-of-the-Art Lithium-Ion Batteries for Electric Vehicles Up to 2030," Licensee MDPI, Basel, Switzerland, September 2017

30. Andrew Burke. "Review of Ultracapacitor Technologies for Vehicle Applications". Institute of Transportation Studies, University of California, California, 2010.

31. Andrew Burke. "Electric Double Layer Capacitors". Key Facts & Benefits, RUSOL GmbH & Co. KG, Germany, 2010.

32. K. Sahay, B. Dwivedi, "Design and analysis of supercapacitors energy storage system for energy stabilization of distribution network," Electrical Power Quality and Utilisation. Journal. Vol. 15, iss. 1, pp. 25-32, 2009

33. M. Ehsani, Y. Gao, A. Emadi, "Modern Electric, Hybrid Electric, and Fuel Cell Vehicles", 2nd ed.; CRC Press: Boca Raton, FL, USA, 2010; pp. 384–385.

34. Mehrdad Ehsani, Yimin Gao, Sebastien E. Gay, Ali Emadi, "Modern Electric, Hybrid Electric, and Fuel Cell Vehicles: Fundamentals, Theory, and Design," (CRC Press, 2004), 239-257, ISBN: 978-1-4200539-8-2.

35. Karin Jonasson, "Analysing Hybrid Drive System Topologies," Department of Industrial Electrical Engineering and Automation, Lund University, Sweden, 2002.

36. Harshit Coutinho, "AVL CRUISE training course," AVL Powertrain Engineering, Inc., Michigan, USA, 2016.

APPENDICES

Appendix A

1 AVL Driving Performance and Consumption Calculation Result for City Hybrid

*** CHARACTERISTIC DATA ***

Curb Weight   <kg>: 23000.0

Admissible Weight   <kg>: 25000.0

Wheel Base   <m>:   5.650

Driving resistance   : Function without Reference Vehicle

Frontal Area   <m2>:   10.750

Lift Coefficient Front <->:   0.000

Lift Coefficient Rear   <->:   0.000

   Engine:

Displacement   <l>:   8.478

Cylinder Number   <->:   8

Stroke Number   <->:   4

Hot Start:	Hot Start - steady state	Load State Empty:	Yes
Location:	Chassis Dynamometer	Load State Half:	No
Gear Sel. Upshifting:	According to Profile	Load State Full:	No
Gear Sel. Downshifting:	According to Profile	Vehicle Mass:	3115.0 <kg>

Vehicle Additional Load: 115.0 <kg>

*** RESULTS ***

Overall Fuel Consumption: 2.5769   [kg]

Idle Fuel Consumption: 0.8543   [kg]

Acceleration Fuel Consumption: 0.7127   [kg]

Constant Drive Fuel Consumption: 0.2132   [kg]

Deceleration Fuel Consumption: 0.7967   [kg]

Overall Energy Consumption: 1.6195   [kWh]

TRANSPORT EFFICIENCY RESULTS:

Fuel Consumption: 25.808 <l/100km>

Appendix B

2 AVL Driving Performance and Consumption Calculation Result for Highway Hybrid

*** GENERAL SETTINGS ***

Hot Start:	Hot Start - steady state	Load State Empty:	Yes
Location:	Chassis Dynamometer	Load State Half:	No
Gear Sel. Upshifting:	According to Profile	Load State Full:	No
Gear Sel. Downshifting:	According to Profile	Vehicle Mass:	23115.0 <kg>
Vehicle Additional Load:	115.0 <kg>		

Overall Fuel Consumption: 0.9671   [kg]

Idle Fuel Consumption: 0.1722   [kg]

Acceleration Fuel Consumption: 0.1899   [kg]

Constant Drive Fuel Consumption: 0.1999   [kg]

Deceleration Fuel Consumption: 0.4050   [kg]

Overall Energy Consumption: 1.6255   [kWh]

TRANSPORT EFFICIENCY RESULTS:

Fuel Consumption: 10.553 <l/100km>

VITA AUCTORIS

NAME:	Zicheng Tang
PLACE OF BIRTH:	Nanjing, China
YEAR OF BIRTH:	1992
EDUCATION:	High School Affiliated to Nanjing Normal University Jiangning Campus, Nanjing, China, 2010
	University of Windsor, B.App.Sc., Windsor, ON, 2015